NTNU
Norwegian University of
Science and Technology

Optimum Configuration of the Dogger Bank Reference Wind Farm Grid with Consideration for Reliability

Vigdis Andrea Gustavsen

Master of Energy and Environmental Engineering
Submission date: June 2016
Supervisor: Gerd Kjølle, ELKRAFT

Norwegian University of Science and Technology
Department of Electric Power Engineering

Problem Description

SINTEF Energy Research has previously developed a reliability model based on the RELRAD methodology for radial power grids that has been applied to offshore wind farms. This master thesis aims to use this methdology along with technical and economical analysis to find the optimum configuration of the Dogger Bank Reference Wind Farm Grid. An evaluation of the factors that influence the reliability should also be performed.

Preface

This thesis was written in collaboration with SINTEF Energy Research during the spring of 2016 at the Norwegian University of Science and Technology (NTNU), at the Department of Electric Power Engineering. The main objective has been to find the optimum configuration of the Dogger Bank Reference Wind Farm using the RELRAD methodology as well as power flow analysis and economic analysis.

I would like to thank my supervisor professor Gerd Hovin Kjølle for excellent guidance, and many interesting discussions on the subject of reliability. The same goes for my co-supervisor Iver Bakken Sperstad at SINTEF, which has had valuable information on issues concerning offshore wind farms. This thesis has really sparked my interest in this field, and look forward to be working on it again some day.

I would also like to thank my fellow students for five memorable years at *Energi og miljø*. Last but not least Bjarne deserves a huge thank you for always supporting me during the production of this thesis and keeping my stress levels down.

Vigdis A. Gustavsen

Vigdis Andrea Gustavsen

Trondheim, June 15, 2016

Sammendrag

Offshore vindkraft har blitt en stor del av den europeiske energimiksen, og ny og forbedret teknologi muliggjør bygging av vindparker med større installert kapasitet. En av disse store prosjektene som har blitt innvilget i Storbritannia er Doggerbank Creyke Beck A med en installert effekt på 1,2 GW. Fra tidligere arbeid har et grunndesign for dette prosjektet kalt Doggerbank Reference Wind Farm, DRW, blitt utviklet av Kirkeby ved SINTEF.

Denne avhandlingen har vurdert seks konfigurasjoner basert på en del av dette grunndesignet med ulik utforming av redundans for å minimere produksjonstapene. RELRAD-metoden, lastflytanalyse og økonomiske vurderinger har blitt brukt for å avgjøre hvilken som er den optimale konfigurasjonen for DRW. Faktorer som tidsvarierende kraftproduksjon, ulike nivåer av redundans, og kostnadene ved effekttap i kabler har blitt vurderert for å avgjøre deres innflytelse på påliteligheten og den økonomisk beslutning for samlenettet. Ved analysen av samlenettets utforminger, har bare komponenter som endres i antall eller plassering blitt evaluert. Dette inkluderer 66 kV PEX-kabler, effektbrytere og lastskillebrytere.

To av konfigurasjonene, som kun tilbyr noe eller ingen redundans, viste seg å ha mye større årlige avbrudd enn de andre, noe som indikerer at disse ikke er den optimale løsningen. For alle konfigurasjoner gir de forventede avbruddskonstandene, kostnad ved effekttap og kabelkostnadene store bidrag til de totale kostnadene, som gjorde at design med lange kabler ble uøkonomiske. Den optimale konfigurasjonen for Dogger Bank referansevindpark ble funnet til å være ”multi ringkonfigurasjonen med full redundans, hvor to ganger tre strenger er koblet til en redundans-kabel, og fire strenger er koblet til en redundans-kabel. For alle sensitivitetsanalyser var det fremdeles ”multi-ringkonfigurasjonen som var den beste løsningen.

For videreføring av dette resultatet bør en full pålitelighetsanalyse av DRW bli utført for å finne de faktiske kostnadene for DRW. I tillegg ville det være gunstig å dimensjonere kablene for kortslutningshendelser for å møte gitte sikkerhetskrav for offshore vindparker.

Abstract

Offshore wind energy has become a major part of the European energy mix, and new and improved technology enables the construction of wind farms with larger installed capacity. One of these large scale projects that has gotten granted consent in the UK is the Dogger Bank Creyke Beck A with an installed capacity of 1.2 GW. From previous work a base case of the collection grid for this project called the Dogger Bank Reference Wind Farm, DRW, has been developed by Kirkeby at SINTEF.

This thesis has evaluated six configurations based on a section of this base case with different design of redundancy to minimize the production losses. The RELRAD methodology, power flow analysis and economic evaluations have been used to determine which is the optimum configuration for the DRW. Factors such as time varying power production, different levels of redundancy, and the costs of power loss in cables has been evaluate to determine their influence on the reliability and economic decision for the collection grid. When analysing the grid designs, only components that changed in number or placement has been evaluated. This included the 66 kV XLPE cables, circuit breakers, and disconnectors.

Two of the configurations, which only offered some redundancy or none at all, was found to have much larger annual outage time than the rest, indicating that these would not be the optimum solution. However, for all configurations the expected interruption costs, cost of power loss, and the cables costs all have had huge contributions to the costs, which made the configurations with long cables much more expensive. The optimum configuration for the Dogger Bank Reference Wind Farm was found to be the multi ring configuration with two times three strings connected to a redundancy cable, and four strings connected to a redundancy cable, offering full redundancy. For all sensitivity analysis performed, the multi ring configuration was still found to be the best solution.

To use this result further, a full reliability analysis of the DRW should be performed to find the actual costs of the DRW. Additionally it would beneficial to dimension the cables for short circuit events to meet the security demands for offshore wind farms.

Contents

List of Figures

List of Tables

Nomenclature

DRW	Dogger Bank Reference Wind Farm
NRT	NOWITECH Reference Turbine
PMSG	Permanent Magnet Synchronous Generator
WT	Wind Turbine
XLPE	Cross-Linked Polyethylene Cable
PCC	Point of Common Coupling
WT	Wind Turbine
L_{ij}	Cable number j on string i
DS	Disconnector
CB	Circuit Breaker
P_{aero}	Aerodynamic power
P_{gen}	Power from generator
P_{eawe}	Expected available power from each NRT
η_{rot}	Efficiency from torot to generator
η_{gen}	Efficiency in generator
η_{con}	Efficiency in converter
η_{trafo}	Efficiency in transformer
EAWE	Expected available wind energy
v_i	wind speed interval
$P_{wt}(v_i)$	Power production from wind turbine at the corresponding wind speed interval
$W(v_i)$	The Weibull probability distribution for the corresponding wind speed interval
P_{tot}	Total power a cable should be able to deliver
P_i	Inital power
P_{red}	Redundancy power
I_n	Nominal current
U_N	Nominal voltage
$\cos\phi$	power factor
ω	$\omega = 2\pi f$
ENS	Energy not supplied (from turbine)

λ_s	Interruptions per year
U_s	Unavailability per year/ Outage time per year
r_s	Hours per outage time
SAIFI	System Average Interruption Frequency Index
SAIDI	System Average Interruption Duration Index
CAIDI	Customer Average Interruption Duration Index
ASUI	Average Service Unavailability Index
ASAI	Average Service Availability Index
WAIDI	Wind turbine Average Interruption Duration Index
Customer	A metered electrical service point for which an active bill account is established at a specific location - In this paper one turbine is defined as one customer
EAWET	Expected Available Wind Energy with Turbine failures
EAWEC	Expected Available Wind Energy with Cable failures
EWED	Expected Wind Energy Delivered
EPDR	Expected Power Delivery Ratio
EIC	Excpected Intrruption Cost
NPV	Net present value

1 Introduction

This master thesis will evaluate the optimum configuration for the Dogger Bank Reference Wind Farm by using technological and economical analyses as well as a reliability analysis. The paper will analyse multiple configurations for the collection grid and compare them to each other to find the best solution. All configurations are based on a radial collection grid, with different design of redundancy to minimize the production losses. Additionally, some factors that may influence the reliability of the wind farm will be evaluated.

1.1 Background

During the last 25 years offshore wind energy has grown into a major part of the European energy mix. The technology improves each year, as do the turbine sizes and power production. With new and improved technology, the efficiency and power production increases. The industry continues to develop and adapt to new demands and challenges [30].

In 2008 the UK identified nine development zones for offshore wind power that together could have the capacity to supply a quarter of the electricity used in the UK by 2020. As a result, Forewind was formed and later announced as the development parter for the largest of these zones; Dogger Bank [6].

In previous studies a reference wind farm for the Dogger Bank project has been developed, abbriviated to DRW . The purpose was to create a base case model to use in further research and benchmarking [10]. The DRW is modelled to have an installed capacity of 1.2 GW distributed over 120 wind turbines, rated at 10 MW each. This is above average for the technology today, and might influence the economic decision regarding the collection grid of the wind farm. Typically there have been a tradition of choosing radial collection grids without redundancy cables.

A larger nominal power of turbines leads to increased losses due faults in the components. With increased rated power for new turbine technology, it is important to see whether or not if it will be more economically feasible to go from a typical radial grid without redundancy, to one with redundancy. This is one of the questions this paper will address, using reliability analysis as well as technical and economical analyses.

In the previous project thesis a comparison of different tools to analyse the reliability for the Dogger Bank Reference Wind Farm was made. The two tools used were DIgSilent PowerFactory and the RELRAD Methodology. The aim was to see if both methods could be used for the same wind farm, and produce the same results. The RELRAD methodology provides the user with better control over the calculations, and is not dependent on a third party program to be conducted. The comparison were satisfactory, and the RELRAD methodology is therefore used in this paper to find the optimum configuration of the Dogger Bank Reference Wind Farm.

1.2 Scope & Delimitations

The main focus of this thesis is finding the optimum configuration of the DRW based on the reliability of the wind farm and finding the marginal economical optimum. The thesis considers six different configurations for the DRW, with a basis in a base case developed by Kirkeby at SINTEF.

When analysing the reliability of the different configurations for the DRW, some delimitations and assumptions can be made. Since the DRW is based on the Creyke Beck A section which consists of three similar sections of 40 wind turbines each, only one section is analysed. The distance between the wind turbines are irregular, but an average distance of 1.8 km between the turbines is assumed.

To find the configuration that has the lowest costs and best reliability only the components that differ in numbers for each configuration is evaluated. This means that since the number of HVAC and HVDC transformer stations does not change with different net configurations and the paper only analyse one section, the 132 kV part of the collection grid is not included, i.e. the 132 kV cables, the HVAC 66/132 kV transformers, and the HVDC 132/400 kV transformer are not included. Since the number of the NRTs and their control systems are the same for all configuration designs, they are neglected in the analysis to find the optimum configuration, even though they have a huge impact on the actual reliability analysis and economic evaluation of the DRW. The same goes for the busbars in the system. The components included in the reliability analysis to find the optimum configuration are the 66 kV cables, disconnectors and circuit breakers, as the number and placement of these are different for each configuration.

The redundancy cables in the different configurations are assumed to be connected at one end of the cable and always available as an alternate route for the power should a fault occur. In this way, the cables are energized but there are not power going through them until they are connected at the other end as well. This will influence the reliability for the wind turbines in the connected radial.

The sectioning of a fault is done by opening the closest circuit breaker to cut the power, then opening the closest disconnector. This is assumed to be a remote operation, where both components have a possibility of malfunction. This malfunction is defined as a common cause fault and are included in the analysis. As a demand for the RELRAD methodology only one fault can occur at a time, and is repaired before another one takes place.

In this thesis the security has been neglected, and only the adequacy of the collection grid as been analysed. This mean that the cables has not been dimensioned for short circuit events. To ensure that the cables are designed for the rated power a power flow analysis is performed. The power flow analysis is performed by using a MATLAB-package called MATPOWER, with a manual assurance that the cables satisfy the technical limitations. During the load flow analysis, a power demand equal to the maximum power production of 400 MW for the analysed section is assumed to be located at the main bus bar, PCC.

When performing the economic analysis an assumption of a lifetime equal to 20 years has been assumed, where cables, circuit breakers, and disconnectors only need to be invested in once during that lifetime. I.e. any costs due to damaged components are neglected.

Any maintenance and operation costs including planed shut-downs as well as demolition costs are not included. The cost of lost production as well as the cost of power losses in the collection grids are discounted over the longevity of the DRW.

The time varying power production in this thesis is for simplicity delimited to be a function of probability found by SINTEF for the Dogger Bank platform, and not analysed using a Weibull graph. The annual production found is simplified throughout the analyses as an average power production for each wind turbine of 5.541 MW, instead of 10 MW which is the rated power. When analysing different levels of redundancy, it is assumed that the control systems of the wind turbines is able to reduce the power production continuously.

The Dogger Bank Reference Wind Farm has wind turbines with a rated power of 10 MW which is higher than the standard today, and as such the failure statistics may be under estimated. This is discussed in greater detail by Vefsnmo and Kirkeby and will be addressed in this thesis through sensitivity analysis.

1.3 Document Structure

The paper will start of by introducing the Dogger Bank Reference Wind Farm, and the technical specifications of the system in Chapter 2. After which the different layouts analysed for the wind farm will be presented in Chapter 3. In Chapter 4 the paper will review the power production at the Dogger Bank, while in Chapter 5 it will present and discuss the components essential to the reliability analysis and to finding the optimum configuration. In Chapter 6 the technical analysis is explained and shown how it is implemented in MATLAB. Chapter 7 explains the reliability analyses, while Chapter 8 shows how the cost analysis is performed. Lastly, Chapters 9 and 10 present the results and conclusion of this paper.

2 Electrical System Description

The offshore wind farm analysed in this project paper is the Dogger Bank Reference Wind Farm (DRW) outside the shore of Yorkshire, England. In this chapter a description of the DRW is given.

2.1 Inter Array System

The Dogger Bank project is shown in Figure 1 and consist of four sanctioned sections; Creyke Beck A and B, as well as Teesside A and B. The Dogger Bank Reference Wind Farm assessed in Kirkeby is the Creyke Beck A offshore wind farm, and is the wind farm analysed in this paper.

Figure 1: Map of the Dogger Bank Project [6]

Creyke Beck A is located 131 km from the shore of the UK and cover an area of 515m^2 and is connected onshore to Fraithorpe through a HVDC transformer platform and 400 kV cable. From Kirkeby, and Kirkeby and Tande an electrical grid was decided for the project, and is shown in Figure 2. Here it can be seen that the DRW is divided into three clusters, each cluster have an installed capacity of 400 MW in 40 turbines, which gives a total of 1.2 GW installed capacity for the DRW. All three clusters are connected to the HVDC platform through a 132 kV HVAC cable and transformer substation each; denoted S1, S2 and S3 in the figure. Each cluster is then again divided into ten strings with four wind turbines connected radially (in series) on each string. This design is analysed to be the best solution in Kirkeby and is used as the base case for the DRW.

Since the three clusters have equally large installed capacity, only cluster S3 is analysed in this thesis. The base case configuration of cluster S3 will be evaluated and redundancy cables connecting the strings together will be assessed to find the best economical solution for the DRW.

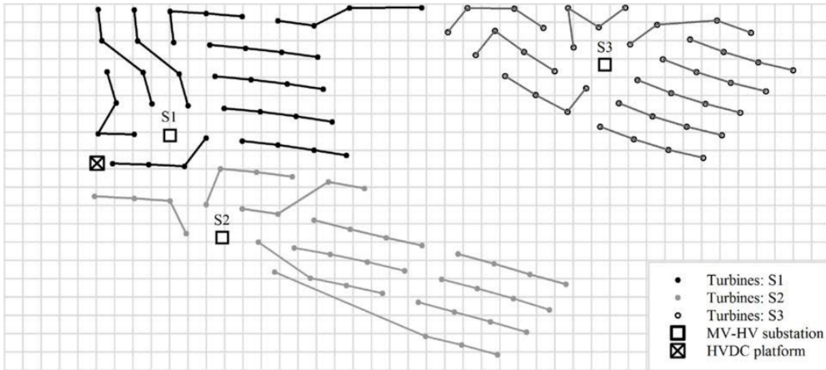

Figure 2: Electrical configuration of DRW [10]

2.2 Technical Specifications

The technical specifications of the wind farm was assessed in *NOWITECH Reference Wind Farm Electrical Design*. In the DRW the wind turbines used are the NOWITECH Reference Turbines (NRT) which are based on the DTU turbine [15] and consist of a 10 MW, 4kV direct drive permanent magnet synchronous generator (PMSG). This is further connected to a 6.5 kV back to back converter, which then is connected to a 11MVA 4/66kV step-up transformer, with Y-Δ connections. The NRT is shown in Figure 3, and is represented as WT in the configuration drawings throughout the paper.

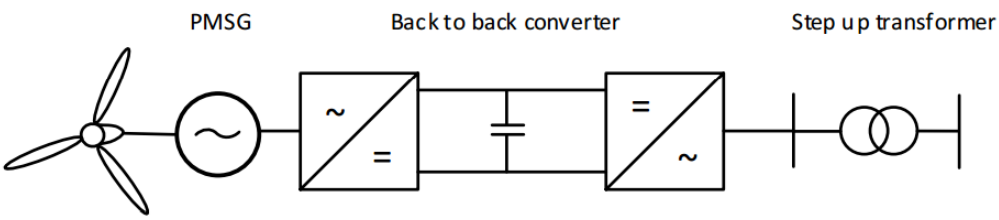

Figure 3: Layout of the NOWITECH Reference Turbine [10]

From the step up transformer in Figure 3, the NRT is connected to the bus bar via a circuit breaker. The bus bar is then connected to a 66kV XLPE cable with disconnectors at both ends. Four NRTs are connected in series in the same matter, and a detailed plan of one of the strings in the collection grid is shown in Figure 4.

Here it can be seen that ten strings are connected to a bus bar or a point of common coupling (PCC). From here the the ten strings are connected to two parallel coupled 66/132 kV, 220 MVA HVAC transformers. The transformers are overrated[1] by 10% to accommodate a level of reactive power flow.

[1]40 turbines x 10 MW = 400MW, 2 x 220MW = 440MW

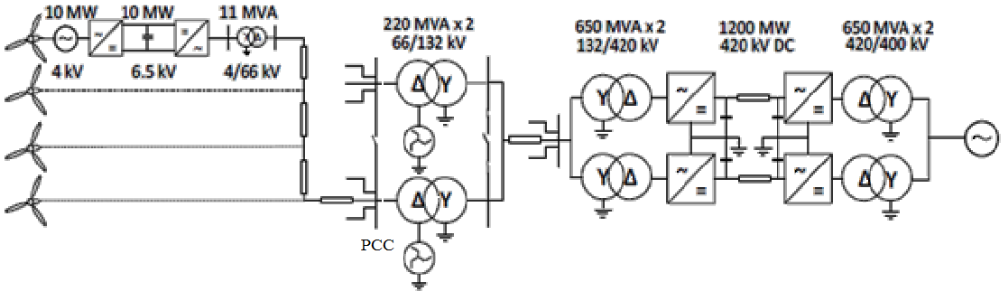

Figure 4: Example of one string in the base case study [29]

After the HVAC transformers there is one 132 kV HVAC cable going from each of the three HVAC sub-platform to the HVDC transformer platform. This platform consists of two parallel coupled 650 MVA 132/420 kV HVAC transformer connected to a 1200 MW 420 kV rectifier, which again is connected to two parallel coupled 650 MVA 420/400 kV HVDC transformers. From this transformer platform, the power is distributed onshore through a 400 kV HVDC cable.

In *NOWITECH Reference Wind Farm Electrical Design* the electrical design for the base case of Dogger Bank is given, but does not go into detail about the placement of disconnectors. This is addressed in “Optimal redundans i Dogger Bank referansevindpark” and is the same design used in this paper.

A more thorough description of the cables, circuit breakers and disconnectors are given in Chapter 5.

3 Alternative Layouts of the Wind Farm

In this chapter, the different designs of the collection grid are presented. These layouts are the same used by Vingdal, as it is of interest to see whether or not the papers reach the same conclusion.

In Figures 7 - 12 detailed sections of the configurations are shown. Here the NRTs are represented as AC voltage sources with the notation for wind turbines, WT. Additionally, all the cables are named L_{ij}, where ij changes depending on the string and turbine number, all disconnectors are noted by DS_{ij} in the same way. Finally, the circuit breakers are noted with CB if they are connected to a NRT, and CBs if they are connected to the point of common coupling, PCC. To better see the distinction between the disconnector and circuit breakers in the figures, they are presented in Figures 5 and 6, respectively. To see the full scale for all configuration, see Figures 30 - 35 in Appendix A.

Figure 5: Symbol of Disconnector

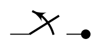

Figure 6: Symbol of Circuit Breaker

3.1 Base Case

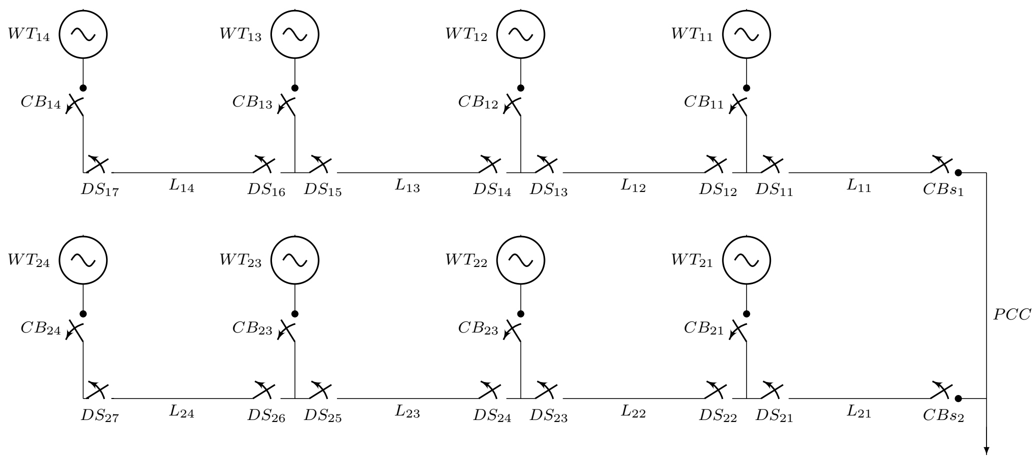

Figure 7: Section of the Base Case Configuration

Figure 7 shows two strings of the base case established in *NOWITECH Reference Wind Farm Electrical Design*. This configuration has no redundancy in the collection grid and is the simplest configuration, with no additional components.

3.2 Multi-Ring

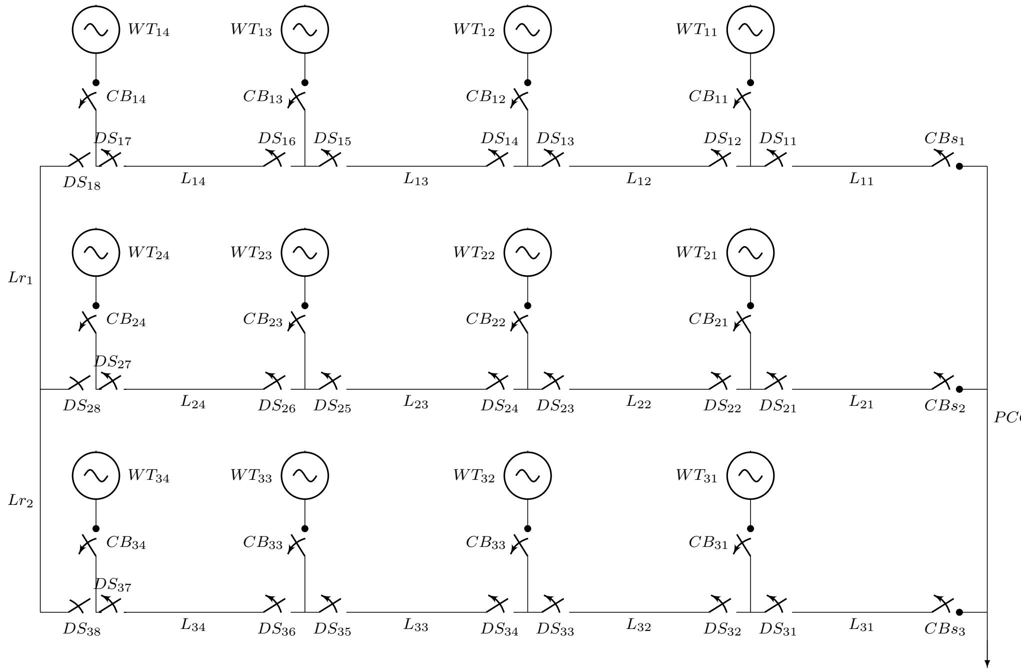

Figure 8: Section of Multi-ring Configuration

Figure 8 shows one of two part of the multi-ring configurations where three strings are connected through two redundancy cables. Additionally, the multi-ring configuration has one part consisting of four strings connected to each other, see Figure 31 in Appendix A for full configuration.

The redundancy cables are noted Lr_1 and Lr_2, and will provide an alternate route for the power if a fault should occur in one of the strings. The cables are initially connected to the rest of the grid at one end of the cables, keeping the redundancy cables energized and ready to be used instantly. If a fault occurs on cable L_{13} the circuit breaker CBs_1 will cut the power distribution to string 1, and disconnector DS_{11} will section out the faulty cable. At the same time, the redundancy cables are connected at the other end as well, and the power generated at WT_{11} - WT_{14} will now flow from string 1 to the PCC trough string 2 and 3. The power is assumed to be approximately divided equally between the two alternate routes.

3.3 Double Ring

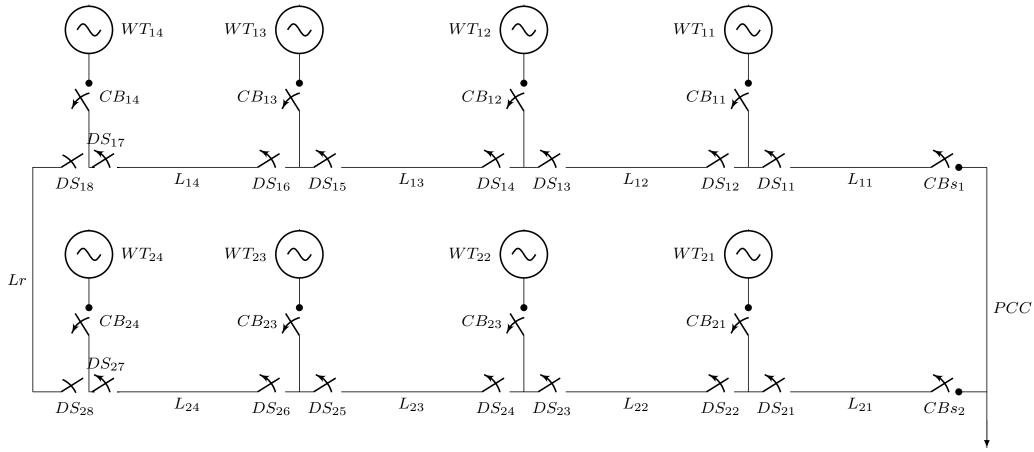

Figure 9: Section of Double Ring Configuration

In Figure 9 one of five parts of the double ring configuration is shown. This configuration looks similar to the multi-ring configuration, except here only two and two strings are connected via the redundancy cables. This configuration offers full redundancy as well, but here all the power produced in the event of a failure in one string, will have to go through the other one. I.e. the functioning cables get a larger strain upon them during a fault, and larger cross-section for the cables are needed.

3.4 Single Ring

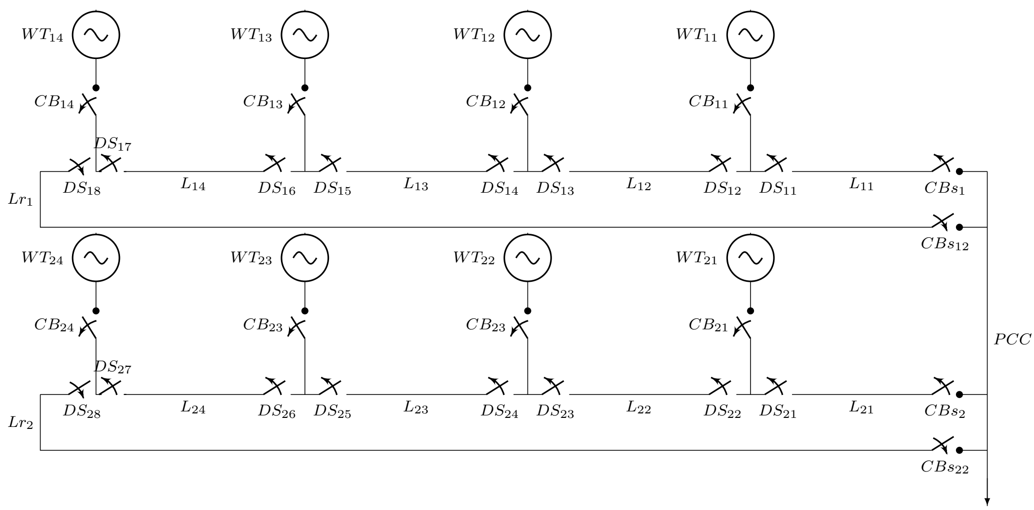

Figure 10: Section of Single Ring Configuration

In Figure 10 two strings of the single ring configuration is shown. This configuration is same as the base case with a redundancy cable at each string going from the wind turbine furthest from the sub-platform to the PCC. This add an extra disconnector near the turbine as well as an extra circuit breaker at the PCC. While most cables are assumed to be 1.8 km long, the redundancy cables of the single ring configuration is assumed to be four times as long, since it would have to cover the same distance as between all four wind turbines.

3.5 Single-Shared Ring

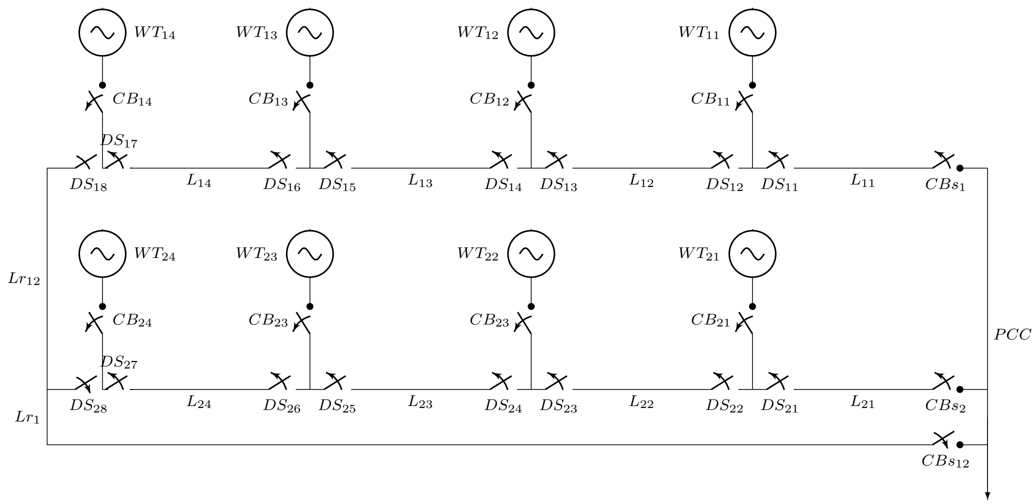

Figure 11: Section of Single Shared Configuration

Figure 11 shows a section of two strings of the single-shared ring configuration. This configuration is a mix between the single ring and the double ring configuration. Two string are connected through a redundancy cable Lr_{12} and to the PCC through Lr_1. Again an additional circuit breaker CBs_{12} is needed, as well as disconnectors to connect and disconnect the redundancy cables. In an event of failure, the power from the faulty string will assumingly go through the long redundancy cable, so that an additional increase in cross-sections for the strings would not be necessary.

3.6 Double-Shared Half-Ring

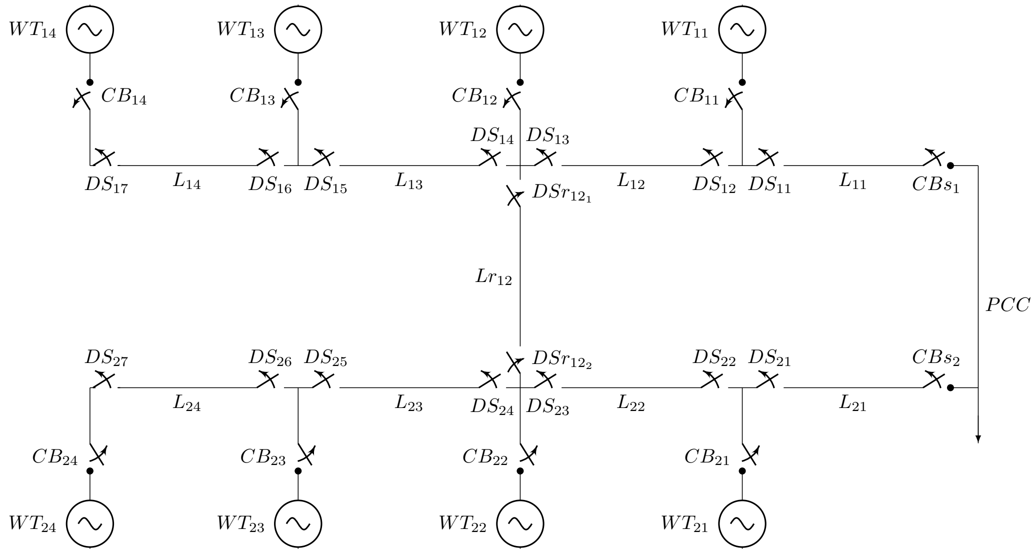

Figure 12: Double Shared Half-Ring Configuration

Lastly, Figure 12 shows the configuration of the Double-Shared Half-Ring. This is similar to the double ring as it has only one redundancy cable between two string, but in this case it is connected half way at the strings. This results in no redundancy in the two outermost wind turbines at each string, given a fault beyond the redundancy cable. It does offer full redundancy if cables 1 or 2, closest to the PCC experience any faults.This is the only configuration that gives some, but not full redundancy of the collection grid. This translates to that all turbines that are the two closes to the PCC on each string, has full redundancy, whilst the two furthest from the PCC only have redundancy for faults before the redundancy cable.

For all configurations with redundancy, the cables are connected at one end at all times to remain energized and available in case of failures.

4 Power Production

The Dogger Bank Reference Wind Farm is designed with wind turbines with a nominal power of 10MW. However, the actual power production is determined by the wind at the Dogger Bank site. This will be addressed in this chapter, as well as how the choice of redundancy influence the results.

4.1 Time Varying Power Production

To account for the actual power production, SINTEF has found a probability distribution based on the wind speed distribution at the Dogger Bank platform [29], which is shown in coloumn two in Table 1.

Table 1: Time variable production

Level	Prob.	Time [h]	P_{aero} [MW]	P_{gen} [MW]	P_{eawe} [MW]	$EAWE_1$ [MWh]	$EAWE_{40}$ [MWh]
1	0.33064	2896.41	10.6000	10.0000	9.3449	27066.5	1 082 661
2	0.03630	317.99	10.0000	9.4340	8.8159	2803.4	112 134
3	0.04816	421.88	8.9440	8.4378	7.8850	3326.5	133 061
4	0.05037	441.24	7.8890	7.4425	6.9549	3068.8	122 751
5	0.05300	464.28	6.8330	6.4463	6.0239	2796.8	11 1871
6	0.05623	492.57	5.7780	5.4510	5.0938	2509.1	100 364
7	0.06035	528.67	4.7220	4.4547	4.1629	2200.8	88 031
8	0.06590	577.28	3.6670	3.4594	3.2328	1866.2	74 650
9	0.07402	648.42	2.6110	2.4632	2.3018	1492.5	59 702
10	0.08789	769.92	1.5560	1.4679	1.3718	1056.1	42 245
11	0.09069	794.44	0.5000	0.4717	0.4408	350.2	14 008
12	0.04645	406.90	0.0000	0.0000	0.0000	0.0	0
SUM	**1**	**8 760.00**				**48 536.9**	**1 941 477**

Column three shows the probability distribution transformed to hours per year when the accompanying wind speed distribution is available at Dogger Bank. Column four shows the aerodynamic power, where $P_{aero} = 10.6\ MW$ is the maximum power generated in the NOWITECH Wind Turbines [10]. For each level the aerodynamic power is assumed to be approx. 1.056 MW lower than the last, until it reaches zero at level 12 [29]. To find the actual power generated, Table 1 accounts for the losses due to the efficiency in the NRT. The efficiency for the different parts of the NRT is shown in Table 2.

Table 2: Efficiency of the NRT

Component	Abbriviation	Effieciency [%]
Rotor to generator	η_{rot}	94.34
Generator	η_{gen}	96.00
Converter	η_{con}	97.90
Transformer (4/66 kV)	η_{trafo}	99.43

Using the efficiency from the rotor to the generator, the power at the generator $P_{gen} = P_{aero} \cdot \eta_{rot}$ in column five is found. To find the expected available power from each NRT P_{eawe}, the rest of the efficiencies are included as shown in Equation (1):

$$P_{eawe} = P_{gen} \cdot \eta_{gen} \cdot \eta_{con} \cdot \eta_{trafo}. \tag{1}$$

To find the power production from this probability distribution, Equation (2) is used [17].

$$EAWE = 8760 \cdot \sum_{v_i=0}^{n} P_{wt}(v_i) \cdot W(v_i) \tag{2}$$

Here, EAWE stand for the expected available wind energy from one NRT, and is shown in column seven in Table 1. 8760 is the number of hours during one year and v_i is the wind speed interval at the Dogger Bank, and is represented as the production level in column one in Table 1 for this thesis. Hence, the power produced by the wind turbine, $P_{wt}(v_i)$ is equal to P_{eawe}, and the Weibull-distribution $W(v_i)$ corresponds to the probability distribution from SINTEF in Table 1. The EAWE for all 40 turbines is shown in column eight.

During the analyses an average production based on the time varying production is used for simplifications. This average production is $P_{avg} = \frac{48536.9\ MWh}{8760\ h} \approx 5.541\ MW$.

4.2 Redundancy

The redundancy is the ability of a system to produce the same amount of power during a fault as when there are no faults in the system. Of the configurations presented in this thesis, the base case is not able to give any form for redundancy, and the double shared half ring configuration enables partly redundancy of the system. The other four configuration all have the ability to offer full redundancy.

When deciding the optimum configuration for the Dogger Bank Reference Wind Farm, one aspect that could change the outcome could be the level of redundancy. To account for a change in redundancy, the cables of the collection grids are designed to withstand a power equal to:

$$P_{tot} = P_i + P_{red} \tag{3}$$

Where, P_{tot} is the total power a cable should be able to deliver, P_i is the initial power a cable is to deliver without a fault in the system, and P_{red} is the maximum power a cable should be able to deliver during a fault *in addition* to the initial power. Tables for cable selections for each level of redundancy examined is given in Appendix B, for all configurations except the base case.

For the double-shared half-ring contribution, which does not offer full redundancy in the first place, the redundancy level focuses on changing the redundancy for those cables that should offer redundancy in the system. I.e. The two cables closest to the PCC for ach string.

5 Components

In this chapter, a more detailed explanation of each component crucial to the reliability will be presented, as well as an example of how a fault in the collection grid might be sectioned out from the rest of the system. The components discussed are the cables, disconnectors and circuit breakers.

5.1 Cable Specifications

To determine the size of the cables to be used, the nominal current needed to deliver the generated power is found. Using Equation (4), the nominal current for each cable section can be found.

$$I_n = \frac{P_{tot}}{\sqrt{3} \cdot U_N \cdot 0.88 \cdot \cos\phi} \tag{4}$$

Here, the notation P_{tot} establish the total amount of power a cable should be able to deliver given any fault in the system. The number 0.88 is incorporated as a result of the research done by Kirkeby and Merz, and is an *under load ratio* which degrades the thermal load of the XLPE cables. The voltage U_N denotes the nominal voltage of the system, i.e. 66kV. The power factor $\cos\phi$ is set to 0.909 for 66 kV XLPE cables [29].

When the nominal current is found, the corresponding cross-section for the cables are selected from *Submarine Cable Systems: Attachment to XLPE Land Cable Systems - Users Guide*. This manual also include the inductance and capacitance of each cable.

Using the inductance and the capacitance from ABB, the susceptance B, and the inductive reactance X of the cables is given by Equations (5) and (6), respectively.

$$B = \omega C \quad [S/km] \tag{5}$$

$$X = \omega L \quad [\Omega/km] \tag{6}$$

The resistance of the cables are not given in the data sheet, but can be found using the Equations (7) or (8) depending on whether the cables have AC or DC. These equations are described in IEC, Stand. 60287.

The resistance of a DC cable is given by Equation (7), where ρ_{co} is the electrical resistivity of copper at $1.68 \cdot 10^{-8}$ Ωm [7].

$$R_{DC} = \frac{\rho_{co}}{A} \quad [\Omega/km] \tag{7}$$

Which is then used to find the resistance of the AC cables which is given by Equation (8).

$$R_{AC} = R_{DC}(1 + y_s + y_p) \quad [\Omega/km] \tag{8}$$

Here y_p is the proximity effect factor shown in Equation (11), and y_s is the skin effect factor of the conductor, shown in Equation (9).

$$y_s = \frac{x_s^4}{192 + 0.8x_s^4} \tag{9}$$

where

$$x_s = \frac{8\pi f}{R_{DC}} \cdot 10^{-7} \cdot k_s \tag{10}$$

and f is the frequency of the current. The cables are assumed to be round or sector-shaped, which results in a coeffiecient k_s equal to 1 [8].

$$y_p = \frac{x_p^4}{192 + 0.8x_p^4} \cdot \left(\frac{d_c}{s}\right)^2 \cdot \left[0.312\left(\frac{d_c}{s}\right)^2 + \frac{1.18}{\frac{x_p^4}{192+0.8x_p^4} + 0.27}\right] \tag{11}$$

where d_c is the diameter of the cable and s is the distance between cable axes, which can both be found in ABB. Here:

$$x_p^2 = \frac{8\pi f}{R_{DC}} \cdot 10^{-7} \cdot k_p \tag{12}$$

where the coefficient k_p is equal to 0.8 since the cables are round or sector-shaped [8].

The resulting cables impedance values can be found in Table 21 in Appendix C. The failure statistics are for simplifications assumed to be the same for all 66kV cables in this thesis.

In addidtion to finding the impedance values of the cables, the power losses for each configuration must be found as this will be different for each configuration. The power loss of one cable is found using Equation (13):

$$P_{loss} = R \cdot I^2 = R \cdot (\frac{P}{U \cdot \cos\phi})^2 \tag{13}$$

where R is the resistance of the cable found in Table 21 in Appendix C, and I is the nominal current through the cable during normal operation. For simplifications, the power losses are calculated for normal operation only. I.e. even though for some hours during the year the redundancy cables are used, the power losses in these are approximately the same as for the rest of the configuration and will not be included.

5.2 Breaker Specifications

The placement of the circuit breakers and the disconnectors influence the reliability the most of all components. They determine whether or not the system is able to section out the faults that occur.

The circuit breakers are placed at each NRT to cut the power from them if a fault should occur in the turbines them selves. Wind turbines have a large effect on the reliability of the wind farm [18], but is not included in this thesis as the effect of them would be about the same for all configurations, as the circuit breakers will cut the power and prevent them from affecting other load points (wind turbines).

The circuit breakers at each string should be able to cut power from the strings if there occurs any faults. If they malfunction the circuit breaker at the transformer platform cuts the power for the entire section before the fault is sectioned.

The disconnectors are dependant on the circuit breakers to cut the power before they can open and section out parts of the string. Disconnectors are assumed to be more stable than circuit breakers in regards of failure frequency [27]. Reliability statistics for all three components are given in Chapter 7.

5.3 Failure of Components

In this subsection, a description on how faults occur and influence the system is provided.

In Figure 13 a section of the multi-ring configuration is shown. The redundancy cables Lr_1 and Lr_2 are connected to string one, i.e. disconnector DS_{18} is closed, while disconnectors DS_{28} and DS_{38} are open. This causes the redundancy cables to be energized, without any power going through them. This is so the redundancy cables are ready to be used in case of a fault in one of the strings, and this will have an influence on the reliability of the WTs in string three where they are connected.

If a fault occurs on cable L_{32} the circuit breaker CBs_3 cuts the power from the string. Now, the two disconnectors DS_{33} and DS_{32} can section out the faulty cable. Without redundancy, turbines WT_{34}, WT_{33}, and WT_{32} will not be able to deliver power to the PCC. Therefore, the redundancy cables Lr_1 and Lr_2 are connected to string three and two, as well as the already connected string one. When circuit breaker CBs_3 closes again, the power from the previous mentioned wind turbines will be distributed equally between the two redundancy cables. This leads to an increased power delivered through string one and two. WT_{31} is able to deliver power through cable L_{31} again when circuit breaker CBs_3 is closed.

In addition to these types of failures there are so called common cause faults or malfunctions of the breakers, which will lead to a greater outage time of the system. This will be further discussed in Chapter 7.

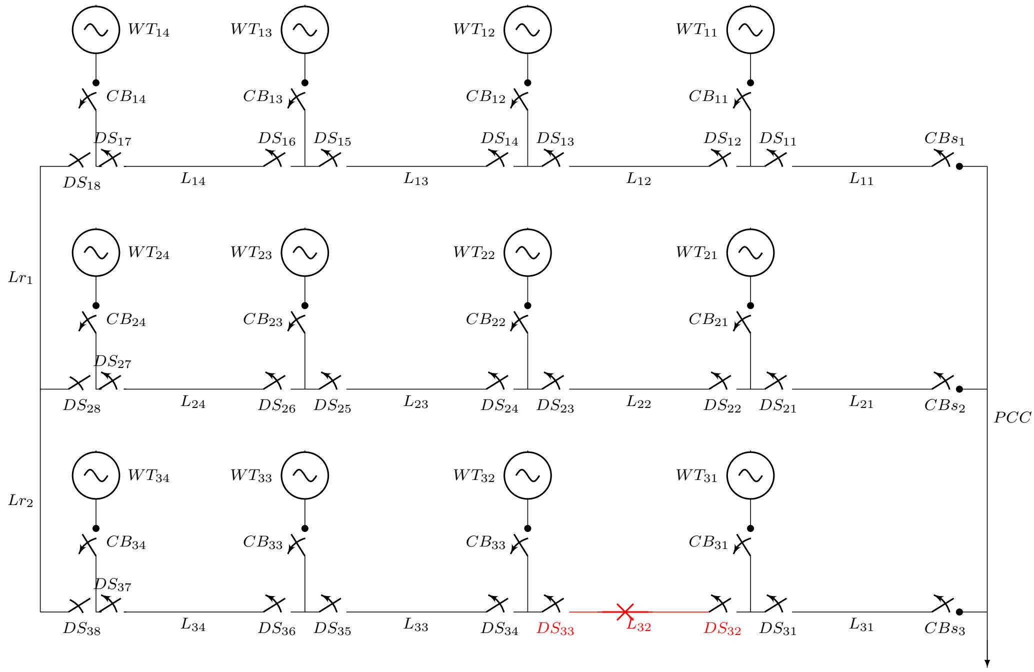

Figure 13: Section of multi ring configuration with failure in L_{32}

6 Technical Analysis

In this chapter, the techincal analysis used in dimensioning the cables is presented. In Vingdal a short circuit analysis was performed to find the maximum current the cables should be able to withstand to meet the requirements of stability during small and large disturbances set by the government [14]. The short circuit analysis has not been included here as it is part of the security of the collection grid, and exceeds the scope of this thesis. The cables are purly dimensioned for rated power and verified through power flow analysis.

6.1 Power Flow Analysis

The power flow analysis examines the state of the system in the planning stage. For instance it can provide information of whether or not the voltages and reactive generations are within upper and lower limits, if the cables experience any overloads, if the voltage angles indicate steady state stability problems, and what the losses in the system are [23]. Not all of this information is necessary in the evaluation of the optimum configurations as there are small differences in the configurations. In this thesis, the main objective of the power flow analysis is to calculate if the cables are able to deliver the produced power during a fault.

The power flow analysis uses information about the active and reactive power for each bus bar in the system as well as voltages and voltage angles; P_i, Q_i, U_i, δ_i. From a practical point of view the voltage angles are not known, but are given in relationship to the voltage angle of the selected reference bus bar, called the slack bus. The other bus bars are categorised into P-V buses or P-Q buses, depending on which variables are known. If the voltage and active power are known for a bus, it is called a P-V bus, if the active and reactive power are known, it is a P-Q bus.

To find the unknown variables in the collection grid, the definition of apparent power is used:

$$\boldsymbol{S} = \boldsymbol{U} \cdot \boldsymbol{I}^* \tag{14}$$

By substituting the current in Equation (14), with the bus voltages and the accompanying node admittance matrix, the apparent power can be presented in therms of active and reactive power as shown in Equations (15) - (17).

$$\begin{bmatrix} P_1 + jQ_1 \\ P_2 + jQ_2 \\ \vdots \\ P_n + jQ_n \end{bmatrix} = \begin{bmatrix} U_1 & & & \\ & U_2 & & \\ & & \ddots & \\ & & & U_n \end{bmatrix} \cdot \left(\begin{bmatrix} Y_{11} & Y_{12} & \cdots & Y_{1n} \\ Y_{21} & Y_{22} & \cdots & Y_{2n} \\ \vdots & \vdots & \ddots & \vdots \\ Y_{n1} & Y_{n2} & \cdots & Y_{nn} \end{bmatrix} \begin{bmatrix} U_1 \\ U_2 \\ \vdots \\ U_n \end{bmatrix} \right)^* \tag{15}$$

$$P_i = Re(S_i) = \sum_{j=1}^{n} Y_{ij} U_i U_j cos(\delta_i - \delta_j - \theta_{ij}) \tag{16}$$

$$Q_i = Im(S_i) = \sum_{j=1}^{n} Y_{ij} U_i U_j sin(\delta_i - \delta_j - \theta_{ij}) \tag{17}$$

Using Equations (16) and (17) and substituting the know variables, a set of equations are found for all bus bars, i. By inserting these equations into each other the unknown variables are found for all bus bars.

6.2 MATPOWER

The power flow analysis is performed using MATPOWER. MATPOWER is a package of M-files for MATLAB aimed to solve power flow and optimal power flow problems [33]. The package uses input on the generators, bus bars, and cables for the power flow analysis, as well as generation cost data for the optimal power flow analysis. In this paper, only power flow analysis is considered as this provides enough information on the power flow during a fault and whether or not the system is able to maintain the power flow in the collection grid.

First, the system apparent power base value is set to 400 MVA, since the wind farm section is to produce 400 MW at the most. Secondly, the bus data is implemented. There are three different types of bus bars; slack bus, P-V bus, and P-Q bus, which are coded as 1, 2, and 3, respectively. All bus bars connected to generators are modelled as P-V buses, while the PCC is defined as the slack bus, or reference bus. The base voltage at all buses are set to 66kV, and the voltage angle at the slack bus is set to zero degrees. An upper and lower voltage limit of 10 % is set, and the slack bus is coded to have a 400 MW active power demand.

Next, the generator and cable data are implemented. The generators are represented as 10 MW generators at each P-V bus. The cables are represented as lines between each bus bar. To implement the cables in MATPOWER, they are first transformed to a pi-equivalent.

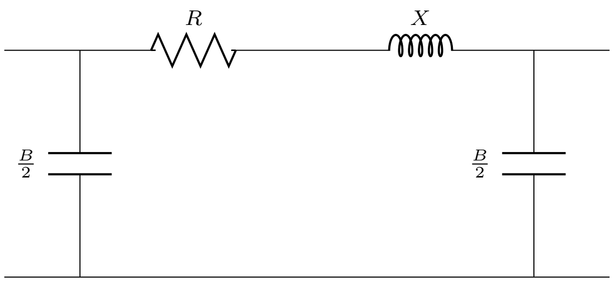

Figure 14: PI-equivalent for Transmission Line

Where R in Figure 14 is given by Equation (8) for the chosen cable cross-section, X is the inductive reactance given in Equation (6) and $\frac{B}{2}$ is the capacitive reactance from Equation (5). For values for all the cross-sections available from ABB, see Table 21 in Appendix C.

In this table, the per unit values are also given. This is necessary as MATPOWER operates in per unit. First, the base values are found in Equation (18) and (19).

$$Z_{base} = \frac{U_{base}^2}{S_{base}^*} = \frac{(66kV)^2}{400MVa} = 10.89\ \Omega \tag{18}$$

$$Y_{base} = \frac{1}{Z_{base}} = \frac{1}{10.89\ \Omega} \approx 0.0918\ S \tag{19}$$

Where U_B is the base value for the voltage of the system, and S_B is the base value of the power of the system. The resulting m-file are shown in Appendix D for the base case as an example. A cable is set to status 1 if the cable is connected to the collection grid, but if a fault occurs and the cables is sectioned out the status is set to zero and the redundancy cables set to 1. The rest of the data is either set to zero or to standard value as defined in *MatPower 5.1 User's Manual*.

7 Reliability Analysis

Reliability of an item is the probability that the item will survive time t [26], and may be measured by the frequency, duration, and magnitude of adverse effects on the electric supply [25].

Vadlamudi divides reliability of a system into two parts; adequacy and security. Whilst security looks at the stability characteristics of the system, adequacy looks at the ability to supply the demanded power to the customers. In this thesis the security of the system is not analysed, but the terms reliability and adequacy is used interchangeable.

7.1 RELRAD Methodology

In this project the RELRAD methodology is used to obtain the reliability of the offshore wind farm. RELRAD is an analytical approach for assessing reliability in radial systems. The methodology is designed to analyse a distribution system and the reliability analysis and the accompanying indices are made for load points, i.e. they consume power [13]. The DRW has a collection system and the ”load points” are the NRTs producing power. To accommodate for this the NRTs will be modelled so that they ”consume” a negative power. When doing so, it is necessary to be aware of the definitions of the indices, as some may need to be redefined.

The model is based upon the primary indices such as expected number of faults (λ_i), mean time to repair (MTTR), and sectioning time. The model uses the fault contribution from all components in the grid and calculate their impact on the defined load points in the system. The load point interruption duration will depend on the protection system of the grid; if the component can be isolated or if it is necessary to wait for the component to be repaired. The topology for the RELRAD methodology is given by equations (20) - (24):

$$\lambda_s = \sum_{i=1}^{n} \lambda_i \tag{20}$$

$$U_s = \lambda_s r = \sum_{i=1}^{n} \lambda_i r_i \tag{21}$$

$$r_s = \frac{\sum\limits_{i=1}^{n} \lambda_i r_i}{\lambda_s} = \frac{U_s}{\lambda_s} \tag{22}$$

$$P_{interr} = P_{load} \lambda \tag{23}$$

$$ENS = P_{laod} U = P_{load} \lambda r \tag{24}$$

For the equations above, the following denotations are valid:

λ_s	- annual frequency of interruptions [interruptiopns per year]
r_s	- average interruption duration [hours per interruption]
λ_i	- expected number of faults per year for component i
r_i	- average repair or sectioning time for compontent i
U_s	- annual duration of interruptions (unavailability) [hours per year]
P_{interr}	- not delivered power [MW interrupted/year]
P_{load}	- power [MW]
ENS	- energy not supplied [MWh/year]

The fault statistics for the three crucial components for the reliability analysis is given in Table 3.

Table 3: Fault statistics

Component	λ_i [1/yr]	MTTR [h]
XLPE Cable	0.005 [1/km]	2030
Disconnector	0.004	240
Circuit Breaker	0.005	240

Additionally, a sectioning time of 30 minutes is assumed. This implies that the breakers and disconnectors are remotely controlled.

7.1.1 Assumptions & Modifications of the Methodology

When applying the RELRAD methodology the following assumptions are made:

- The distribution system must be operated radially. All mesh-connections are regarded as reserve connections.
- Faults are isolated by the nearest circuit breaker. If the fault occurs in the circuit breaker the second nearest circuit breaker will isolate the fault. Any load points that are dependent on the circuit breaker will experience outage time. A probability of failure to open the circuit breaker (isolate the fault) may be represented in the model.
- All faults are considered statistically independent.
- Each fault is considered to be repaired before the next fault occurs.
- Overlapping faults are not represented.
- Reserve connections are assumed available on demand.

Some disadvantages in using the RelRad methodology is that it does not include overlapping faults and any permanent alternate routes in the grid has to be modelled as a parallel coupling. In this thesis all redundancy is only partly coupled to the radial strings, and a parallel coupling reliability analysis is not necessary.

Usually, the RELRAD methodology is used for distribution grids with load points interrupted by the fault in the components of the grid. This thesis analyses a wind power production system with a collection grid. To be able to use the RELRAD model the assumption that one load point is equal to one turbine is made. Since the turbines are rated at a production of 10 MW, the RELRAD model sees them as load points producing 10MW, and that ENS is defined as the energy not supplied *from* the turbines (load points).

7.1.2 Common Cause Fault

In the RELRAD methodology overlapping faults are not represented, but common cause faults may be. Common cause faults are defined as the probability for the circuit breaker or the disconnector to malfunction. To calculate the corresponding reliability indices, Equation (20) is adjusted and is given as:

$$\lambda_s = \sum_{i=1}^{n} \lambda_i \cdot P_{0i} \tag{25}$$

Where λ has the same denotation as before and P_{0i} is the probability of a failure in the protection system component i. This means that for any given fault, there is a possibility P_{0i} that the closest disconnector to the fault is unable to section out the fault. For load points with additional disconnectors between itself and the fault, this will have no impact on the reliability output. However, if the load point is close enough to experience prolonged outage time due to disconnector malfunction, there will be a total outage time equal to:

$$U_i = \lambda_i \cdot P_{0i} \cdot r_i + \lambda_i \cdot (1 - P_{0i}) \cdot r_i \tag{26}$$

If the circuit breaker fails to cut the power, the next circuit breaker in the collection grid loacted at the transformer platform is opened in stead. This will cause all of the strings in one section to experience an outage time, as the circuit breaker(s) of the faulty string is unable to cut the power. The possibility P_0 for each type of component is given in Table 4.

Table 4: Probability of malfunction of breakers

Component	P_0
Disconnector	0.01902
Circuit Breaker	0.02377

7.2 Customer-oriented indices

In addition to the primary indices used by RELRAD methodology, a continuation can be done to accommodate the indices to the number of customers. These indices describe the reliability of a power system, and are calculated using the Equations (27) - (31). These equations are a result of the work of IEEE Power & Energy Society et al.

The first index is SAIFI (System average interruption frequency index) and gives the average annual interruption frequency for a system:

$$SAIFI = \frac{\sum\limits_{i=1} \lambda_i N_i}{\sum\limits_{i=1}^{n_{tot}} N_i} \tag{27}$$

In other words, SAIFI is the total number of customers interrupted divided by the total number of customers served in the system.

The second index is SAIDI (System average interruption duration index) and gives the average annual duration of interruptions for a system:

$$SAIDI = \frac{\sum\limits_{i=1} U_i N_i}{\sum\limits_{i=1}^{n_{tot}} N_i} \tag{28}$$

I.e. SAIDI is the sum of hours of interruptions for the customers divided by the total numer of customers served in the system.

The third index, CAIDI (Customer average interruption duration index), gives the average annual duration of interruption for one customer:

$$CAIDI = \frac{\sum\limits_{i=1} U_i N_i}{\sum\limits_{i=1}^{n} \lambda_i N_i} \quad (= \frac{SAIDI}{SAIFI}) \tag{29}$$

CAIDI is therefore defined as the sum of hours of interruptions for the customers divided by the total number of customers interrupted. The number of customers at each "load point" is defined as one turbine.

Lastly, the indices ASUI (average service unavailability index) and ASAI (average service availability index) describes the average annual probability of a customer to experience unavailable and available, respectively:

$$ASUI = \frac{SAIDI}{8760} \tag{30}$$

$$ASAI = 1 - ASUI = \frac{8760 - SAIDI}{8760} \tag{31}$$

Or, ASUI is the customer hours service unavailability divided by the customer hours service demand, and ASAI is the customer hours service availability divided by the customer hours service demand.

In equations (27) to (31), the following denotations are applicable:

λ_i	- frequency of an interruptions for "load point" i
N_i	- no. of interrupted customers for each sustained interruption event at load point i
n_{tot}	- total number of customers served in the system
U_i	- annual interruption duration for "load point" i
8760	- hours service demand (all year)

7.3 Energy-oriented reliability indices

Lastly, the reliability of different configurations of the Dogger Bank Reference Wind Farm is presented using energy-oriented indices. These indices is a result of the work done by Negra and Shin et al., and are categorised into different levels depending on what they represent. These indices are presented in Table 5.

Table 5: Reliability Indices

Level	Index	Definition
1: Turbine	EAWE	Expected Available Wind Energy [MWh]
	EAWET	Expected Available Wind Energy with Turbine failures
2: Net configuration	EAWEC	Expected Available Wind Energy with Cable Failures
3: Delivery Point	EWED	Expected Wind Energy Delivered
	EPDR	EPDR = $\frac{EWED}{EAWE}$

The energy-oriented indices compare expected energy produced by the wind farm, with the losses due to interruptions in the system. The level-column in the table explains where in the system the index is obtained. The EAWE has been explained in Chapter 4, and in this thesis both an expected available wind energy for 10 MW per turbine, and an average of 5.541 MW will be analysed. The EAWET describes the expected available wind energy after energy not delivered due to failures in the turbines has been subtracted. These failures are not included in this thesis as they will be approximately the same for all six configurations. At EWED the power losses of the cables has been included as well. This gives the equation:

$$EWED = EAWE - ENS - (P_{loss} \cdot \text{uptime of the turbines}) \tag{32}$$

The EPDR shows the relationship between the expected energy delivered and the expected available wind energy in the system. A higher EPDR means a lower percentage of loss in the configuration.

There are many more energy-oriented indices that could be used but for all intents and purposes for this paper, the EAWE, EAWEC, EWED, and EPDR suffice. EAWET are not included in the analysis, but are included in Table 5 to show that there are failures in the entire system, not just the net configurations. Not shown are expected available wind energy with failures in disconnectors and circuit breakers, but they are extracted from the final value of expected wind energy delivered, EWED.

8 Cost Analysis

In addition to finding the reliability indices for the DRW it is important to put them in an economical perspective to find which configuration is the most profitable. The annual outage time found in the reliability analysis gives information of how much income is lost due to the faults that occur in the system. A higher loss of income gives incentive to invest in redundancy in the system. The relationship between cost of failures and cost of investments is illustrated in Figure 15.

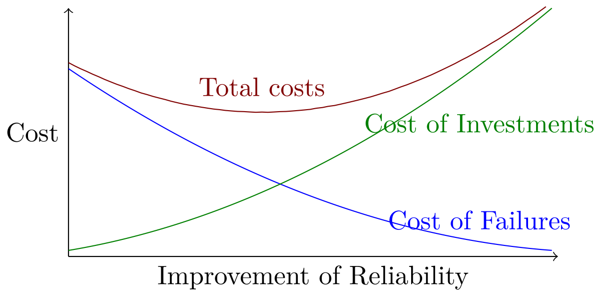

Figure 15: Reliability Cost-Worth [24]

An assumption is made that reliability improvements which result in fewer failures and therefore lower cost of failures, typically occur only with increased investment or operating costs [24]. In this system an increase in investment of redundancy cables and other components will thus give a lower cost of failures.

8.1 Components Cost

For the DRW, cost of investment can be allocated between costs of components and installation costs for cables. The cost of cables are dependant on the cross section of the cable and the nominal voltage of the cable. In *NOWITECH Reference Wind Farm Electrical Design* the costs of a medium voltage (MV) cable can be found using Equation (33):

$$C_{c,MV} = \alpha + \beta e^{\frac{\gamma I_n}{10^5}} \quad [k€/km] \tag{33}$$

Where the cost constants for a 66kV XLPE cable are given as $\alpha = 87.09$, $\beta = 79.11$, and $\gamma = 243.30$ [10].

Use this in Equation (33) to find the cost of each cable per km from ABB, as seen in Table 20.

In addition to the cost of each cable, an installation cost for cables is included. This is based on empirical data from SINTEF Energy Research, and is given as $0.15[M€/km]$ [10]. When comparing the different configurations, the number of circuit breakers and disconnectors will also change and must be included in the cost analysis. The unit price of the 66kV circuit breakers is $\$35,650$ [3], and the unit price for the 66kV disconnectors

Table 6: Three-core cables with lead sheath, nominal voltage 66kV [2]

Cross-section $[mm^2]$	I_n [A]	C_{cable} [M€/km]
95	300	0.251
120	340	0.268
150	375	0.284
185	420	0.307
240	480	0.341
300	530	0.374
400	590	0.419
500	655	0.476
630	715	0.538
800	775	0.608
1000	825	0.676

is approximately $\$47,000$ [22]. Disconnectors have a lifetime of over 40 year [20], while circuit breakers have a lifetime of up to 50 years [5]. Since the lifetime of the wind farm is set to 20 years, there is no need to invest in additional breakers during the lifetime, unless they get broken. This is part of the operation and maintenance costs, and not a part of the scope of this thesis.

Since the Dogger Bank lies outside the UK and interacts with the British electrical grid, all currency are converted to GBP, with 1.00 $USD = 0.6837\ GBP$ [32], and 1.00 $EUR = 0.7602\ GPB$ [31].

8.2 Net present value

The income lost due to faults in the system is defined as expected interruption costs, or EIC, and is found by multiplying ENS with the price of electricityin the UK. The price is set to 150£/MWh since the start of construction of the Dogger Bank Creyke Beck A was last year (2015) [4]. Since the value of life cycle costs is referred to the construction year of the wind farm the cost of expected interruptions are discounted with 9 % per year [10]. To properly calculate the EIC for the lifetime of the wind farm of 20 years, the net present value, or NPV, is found using Equation (34).

$$NPV = \sum_{t=1}^{20} \frac{EIC}{(1+0.09)^t} \tag{34}$$

Where t is the year, and year 1 is defined at the end of year one of the life time.

The same goes for the cost of power losses in the configuration. Since this thesis only seek to find the optimum configuration, the costs that are the same for all configuration are neglected and the total cost can defined as:

$$C_{tot} = C_{DS} + C_{CB} + C_{cables} + C_{installation} + \sum_{t=1}^{20} \frac{EIC}{(1+0.09)^t} + \sum_{t=1}^{20} \frac{C_{P_{loss}}}{(1+0.09)^t} \tag{35}$$

9 Results

Here the results of the reliability analyses and the cost analysis is presented. How a change of redundancy will influence the choice of optimum configuration is also addressed, as well as a qualitative evaluations of the factors that influence the reliability of the system. Lastly, multiple sensitivity analyses are performed to find the validity of the conclusion.

9.1 Reliability Analysis

Here the results of the RELRAD methodology from Chapter 7 is shown, as well as the customer-oriented indices and the energy-oriented indices.

9.1.1 RELRAD Indices

The table below includes both regular faults statistics as well as common cause faults discussed in Chapter 7.

Table 7: Results from the RELRAD methodology

	λ	r	U
Base Case	1.52	1728.78	2621.32
Multi-ring	1.62	384.50	622.61
Double Ring	1.60	388.90	622.57
Single Ring	1.97	317.00	623.30
Single-Shared Ring	1.81	344.90	622.98
Double-Shared Half-Ring	1.60	876.58	1403.49

From Table 7 it can be seen that the base case has the lowest number of faults occurring in the system during one year. This expected as the base case has the lowest amount of components where a fault can occur. Corresponding with this, the single ring configurations has the highest number of components and also the highest number of total faults during on year. Since the Double Ring configuration and the Double Shared Half Ring configuration has the same amount of components, only placed differently, the annual frequency of faults is the same. The index r, shows the average outage time per fault for the configurations.

The annual outage time U is shown in column four. For the four configurations that offer full redundancy, the outage times are quite similar. The differences are a result of different numbers of components which contribute to the fault statistics in the system. The Double Shared Half Ring offers some redundancy and have a larger outage time than the others, but a smaller outage time than the Base Case, which has no redundancy at all. From a reliability point of view, the Double Ring configuration is the best solution. This does not however include the costs of investments, which will be discussed later in this chapter.

9.1.2 Customer-Oriented Indices

The customer-oriented indices relates the primary indices from section 9.1.1 to the number of customers in the system. The results can be seen in Table 8.

Table 8: Results for customer-oriented indices

	SAIFI	SAIDI	CAIDI	ASUI	ASAI
Base Case	0.0379	65.53	1728.78	0.0075	0.9925
Multi-ring	0.0405	15.57	384.50	0.0018	0.9982
Double Ring	0.0400	15.56	388.80	0.0018	0.9982
Single Ring	0.0492	15.58	317.00	0.0018	0.9982
Single-Shared Ring	0.0452	15.57	344.90	0.0018	0.9982
Double-Shared Half-Ring	0.0400	35.09	876.48	0.0040	0.9960

Since the number of customers is defined as one per load point (one turbine is one customer) the total amount of customers is 40. It is then possible to see that the SAIFI and SAIDI is just the primary reliability indices λ_s and U divided by 40. Customer average interruption duration index, CAIDI, will therefore be the same as the average interruption duration for the system, r_s.

These indices shows the same results as before. However, the differences in average system availability index, ASAI, for the four configurations in the middle are so small that ASAI is perceived the same for all. Since the differences are so small, this would suggests that any of these four configurations may be the optimum solution.

9.1.3 Energy-Oriented Indices

The energy-oriented indices assuming an production of 10MW wind power per turbine is given in Table 9.

Table 9: Results for energy-oriented indices

	EAWE [MWh]	ENS [MWh]	P_{loss} [MW]	Uptime [h]	EWED [MWh]	EPDR
Base Case	1 941 477	26 213.21	1.84	6138.68	1 903 996.82	98.07 %
Multi Ring	1 941 477	6 226.11	0.84	8137.39	1 928 429.73	99.33 %
Double Ring	1 941 477	6 225.75	0.34	8137.43	1 932 476.35	99.54 %
Single Ring	1 941 477	6 233.05	1.81	8136.70	1 920 478.37	98.92 %
Single Shared Ring	1 941 477	6 229.85	1.81	8137.02	1 920 480.99	98.92 %
Double Shared Half Ring	1 941 477	14 034.90	0.75	7356.51	1 921 890.97	98.99 %

Uptime is the annual total operational hours, i.e. 8760 hours minus the outage time of the configuration.

The expected available wind energy is calculated assuming time varying production, so a more accurate comparison would be shown in Table 10.

Table 10: Results for energy-oriented indices with time varying production

	EAWE [MWh]	ENS [MWh]	P_{loss} [MW]	Uptime [h]	EWED [MWh]	EPDR
Base Case	1 941 477	14 524.74	1.84	6138.68	1 915 685.29	98.67 %
Multi Ring	1 941 477	3 449.88	0.84	8137.39	1 931 205.95	99.47 %
Double Ring	1 941 477	3 449.69	0.34	8137.43	1 935 252.41	99.68 %
Single Ring	1 941 477	3 453.73	1.81	8136.70	1 923 257.69	99.06 %
Single Shared Ring	1 941 477	3 451.96	1.81	8137.02	1 923 258.88	99.06 %
Double Shared Half Ring	1 941 477	7 776.74	0.75	7356.51	1 928 149.13	99.31 %

The EWED will not be the actual Expected Energy Delivered since the faults of many components are not included in the analysis, and losses in other part of the collection grid is not included. It does however show which configuration will give the highest amount of energy, although the value is not the actual energy delivered. From this analysis the Double Ring configuration has the best ratio of energy delivered to the expected available wind energy.

It can be seen that the production lost due to power losses are close to the value of energy not supplied from the turbines, and must be included in the analysis as this changes for each configuration. The base case, single ring and single shared ring configurations all have a very high power loss in the cables. It might be of interest to increase the cross-section of some of the cables in these configurations as this will decrease the power losses. However, this will also increase the cable costs and make it less profitable. A sensitivity analysis of the cable costs have been performed to address this situation and will be further discussed later in this chapter.

9.2 Cost Analysis

The total cost of each configuration using Equation (35) is shown in Figure 16. It can be seen that the three components that contribute the most to the total cost is the cable cost, the EIC and the cost of power losses in the cables. For the base case the EIC contribute with almost 50 %, but this is assuming a power production of 10 MW per wind turbine. In Figure 17 the corresponding analysis is shown for time varying power production.

For both figures the multi ring configuration is the most profitable solution, with double ring as the next cheapest solution. However, when choosing suitable cables for each configurations, the double ring configuration demands some cables with cross-section of over 1000 mm^2, which is not offered by the manufacturer [2]. See Table 16 in Appendix B. The same goes for the double shared half ring configuration, and both needs a reduction in the level of redundancy to be a real alternative. If the cables are not dimensioned to withstand the rated power, the power flow analysis performed in MATPOWER fails, and the configuration alternative is invalid. For all configuration with all levels of redundancy, with the exception of double ring, and double shared half ring configurations at a redundancy level of 100 % and 90 %, the power flow analysis is valid.

For configurations base case, single ring and single shared ring, the cost of power loss is very high. This is because these cases uses cables with small cross-sections, which gives a high resistance. If cables with larger cross-sections are chosen, the costs of cables increase. A comparison of this is done in section 9.5.

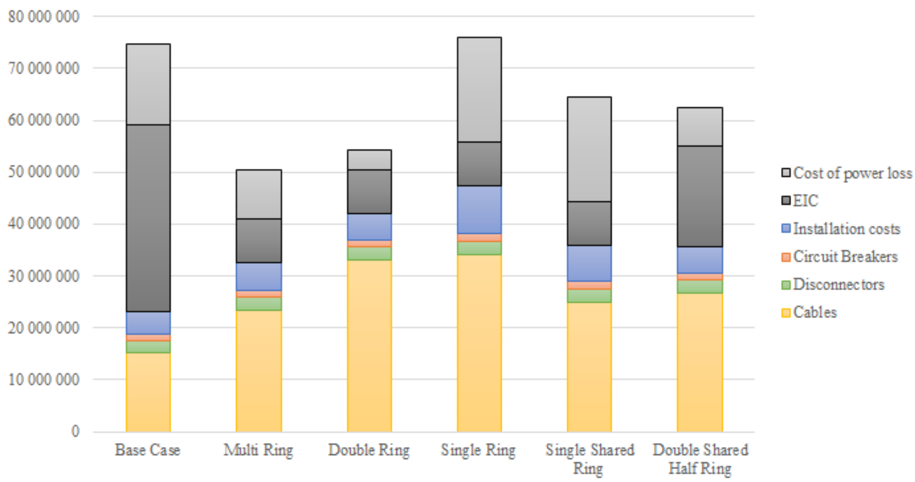

Figure 16: Costs for each Configuration distributed by components

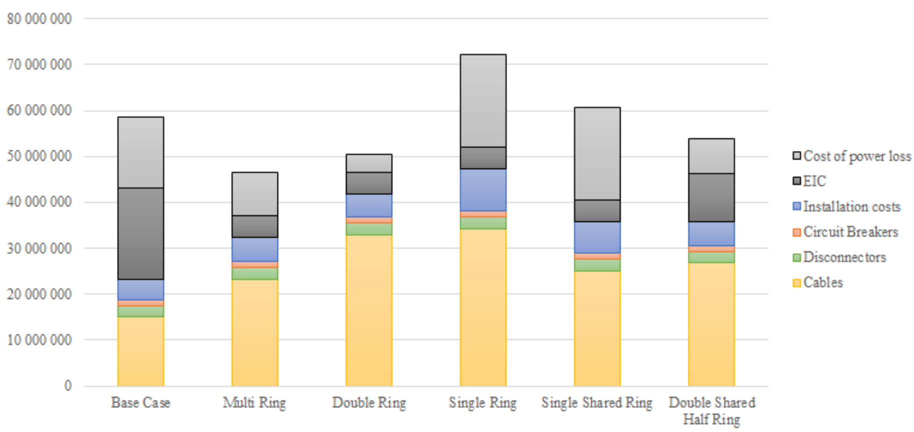

Figure 17: Costs for each Configuration distributed by components with Time Varying Production

9.3 Change of Redundancy

The optimum configuration of the system is found for full redundancy, as is the definition. However, it could be interesting to find the optimum configuration with the optimum level of redundancy. This is done by dimensioning the redundancy cables for a lower power, as well as finding the additional ENS as a cause of this.

Since power losses are dependant of the resistance and thus the cross section of the cable, a reduction in cross section may lead to higher resistance and higher costs of power losses.

When finding the ENS for each case, the first thing to do is finding the amount of time the redundancy cable is in use. For a redundancy of 75% to 99% this means when the cable closest to the PCC experience a fault. The additional outage time for the cable is $U_{cable} = 0.009 \cdot 2030h = 18.27\ h/year$, since the cable(s) are unable to deliver full power during these faults. The corresponding ENS for this time is added for all ten strings and a resulting ENS is given in Table 11. For when the redundancy cables are only designed to deliver 74 % to 50 % of the full production, an outage time equal to $U_{cable} = 0.009 \cdot 2030h \cdot 2 = 36.54\ h/year$ is found. This is because the redundancy cable will be unable to deliver full power when either one of the two cables closest to the PCC expierience a fault.

Table 11: ENS for different levels of redundancy

Lvl. of redundancy	Base Case	Multi-Ring	Double Ring	Single Ring	Single Shared Ring	Double Shared Half Ring
1	26 213.21	6 226.11	6 225.75	6 233.05	6 229.85	14 034.90
0.9	26 213.21	6 956.91	6 956.55	6 963.85	6 960.65	14 765.70
0.8	26 213.21	7 687.71	7 687.35	7 694.65	7 691.45	15 496.50
0.75	26 213.21	8 053.11	8 052.75	8 060.05	8 056.85	15 861.90
0.7	26 213.21	10 610.91	10 610.55	10 617.85	10 614.65	18 419.70
0.6	26 213.21	12 072.51	12 072.15	12 079.45	12 076.25	19 881.30
0.5	26 213.21	13 534.11	13 533.75	13 541.05	13 537.85	21 342.90

In Table 11 the ENS are given for a power production of 10 MW per turbine. A similar result can be found for the time varying production in Table 12.

Table 12: ENS for different levels of redundancy for time varying production

Lvl. of redundancy	Base Case	Multi-Ring	Double Ring	Single Ring	Single Shared Ring	Double Shared Half Ring
1	14 524.74	3 449.88	3 449.69	3 453.73	3 451.96	7 776.74
0.9	14 524.74	3 854.82	3 854.62	3 858.67	3 856.89	8 181.67
0.8	14 524.74	4 259.76	4 259.56	4 263.60	4 261.83	8 586.61
0.75	14 524.74	4 462.23	4 462.03	4 466.07	4 464.30	8 789.08
0.7	14 524.74	5 879.50	5 879.30	5 883.35	5 881.57	10 206.35
0.6	14 524.74	6 689.38	6 689.18	6 693.22	6 691.45	11 016.23
0.5	14 524.74	7 499.25	7 499.05	7 503.09	7 501.32	11 826.10

The ENS of the base case will not differ as there is no level of redundancy to begin with. The double shared half ring configuration is only designed to give full redundancy to four out of eight turbines in one section, and will not have as high a percentage increase in the ENS. The resulting total cost for each configuration can be shown in Figure 18 for a production of 10MW, and in Figure 19 for a time varying production. During this analysis the assumption that all power goes through the original cables has been made to simplify the calculations for the power loss costs, as it would be too time consuming to do otherwise.

For both figures the multi ring configuration at 100 % redundancy is the least expensive of all the alternatives. For a level of redundancy of over 80 % the double ring configuration is cheaper, but still not as cheap as the multi ring configuration at 100 % redundancy. In this analysis the reduction of redundancy has included a reduction of cable cross-section, which decreases the cable costs but at the same time increases the costs of power losses. If the increase in costs of power losses has been greater than the decrease it would have been possible to choose cables with higher cross-sections. This would however still mean that a higher redundancy level would be more profitable.

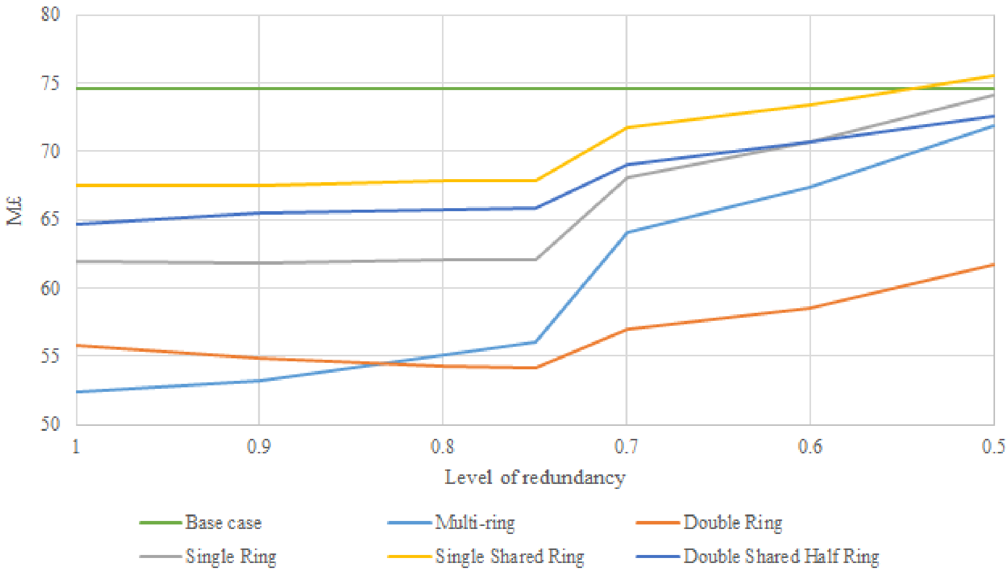

Figure 18: Total cost for each level of redundancy for all configurations

9.4 Qualitative Evaluation of Reliability Factors

When looking at the qualitative effects of reliability factors, the possibility of malfunctioning circuit breakers and disconnectors, or the common cause faults are neglected. The resulting reliability data without the common cause faults are as shown in Table 13.

Table 13: Results for all cases

	λ	r	U
Base Case	1.34	1947.76	2610.00
Multi-ring	1.44	413.51	596.69
Double Ring	1.43	418.72	596.68
Single Ring	1.79	333.44	596.87
Single-Shared Ring	1.62	366.14	596.79
Double-Shared Half-Ring	1.43	838.56	1194.94

From the table it can be seen that there is little difference in the annual frequency of faults in the configurations. The main reason for the small differences that are, could be assigned to a difference in the number of components in the systems. For one wind turbine Figure 20 shows how each type of component contribute to the annual frequency of faults for each

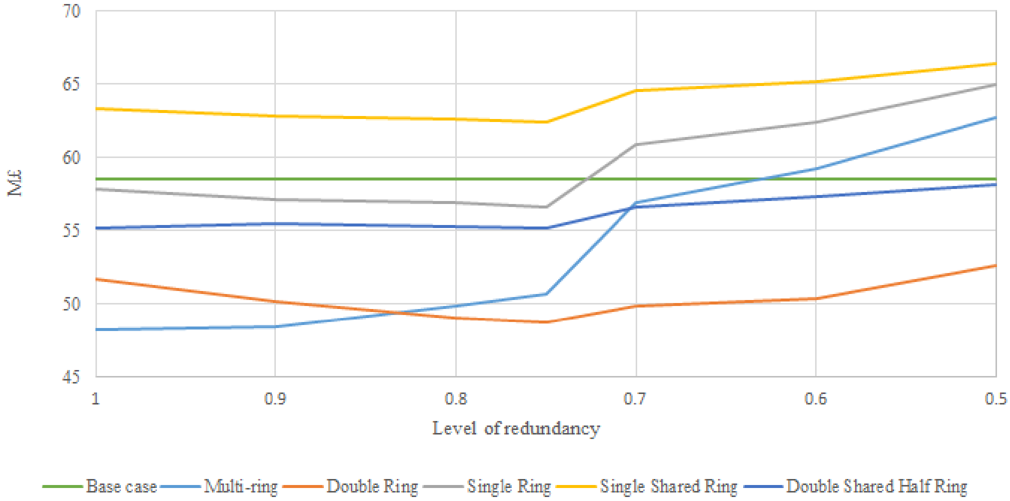

Figure 19: Total cost for each level of redundancy for all configurations with time varying production

configuration. The differences between each configuration is small as would be expected from Table 13. For the single ring and the single shared ring configurations the component with the highest contribution to frequency of failure is the cable. This would be expected as these two configurations have a larger amount of cables in the design. The next highest contributor for these two configurations and the highest for the other configurations are the circuit breakers located at each string. If a fault occurs in any circuit breaker at the string, all other strings will experience an outage time as well. The type of component that contribute the least for all configurations is the circuit breakers connected at each turbine. These will only contribute to an outage time for the other load points at the same string, i.e. one load point (turbine) will only experience failures from circuit breakers for four turbines, while it will experience failures for all circuit breakers for the strings.

In Figure 21 the components contribution to the outage time for each configuration is shown. In the base case configuration the cables contributes to 70 % of the outage time in the collection grid. Since a failure in a cable has such a long mean time to repair compared to the other components, this is to be expected. The double shared half ring offers full redundancy for two out of four cables in a string, and will thus have quite a bit smaller percentage of outage time cause by cables. For the four configurations with full redundancy the outage time caused by cables has almost disappeared. The remaining contribution is due to the sectioning time when a fault in the cables occurs. For these configurations the main contributors are the circuit breakers at each string. If a fault occurs in one of them, the entire section of all ten strings experience an outage time equal to the repair time of the circuit breaker.

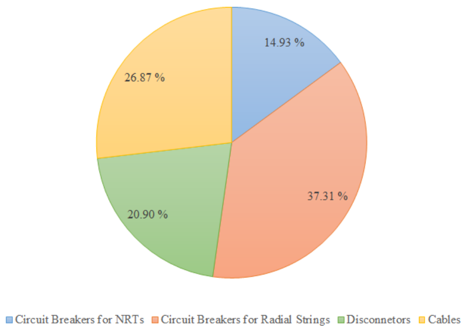

(a) Base Case

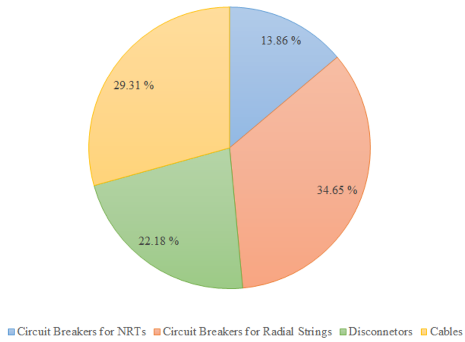

(b) Multi Ring

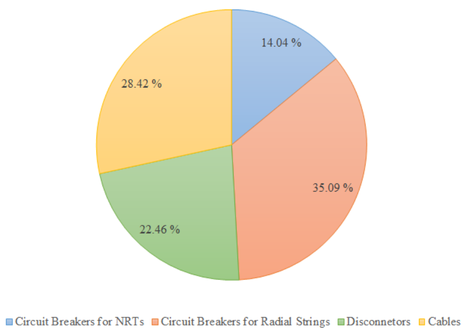

(c) Double Ring

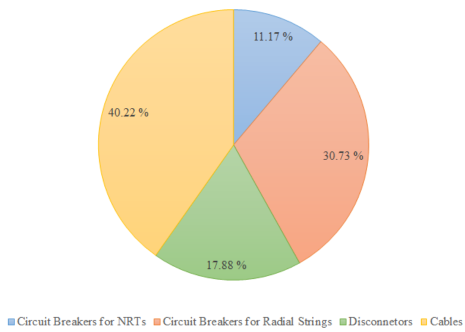

(d) Single Ring

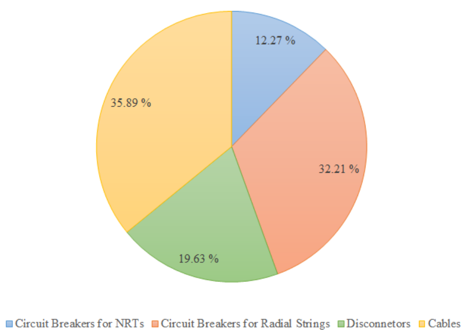

(e) Single Shared Ring

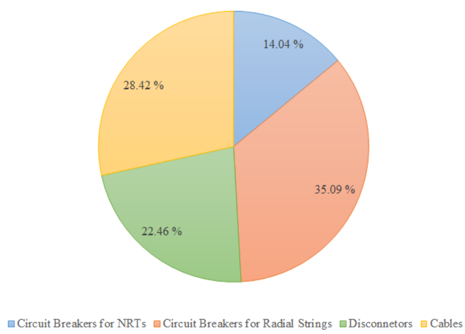

(f) Double Shared Half Ring

Figure 20: Components contribution to frequency of faults for each configuration

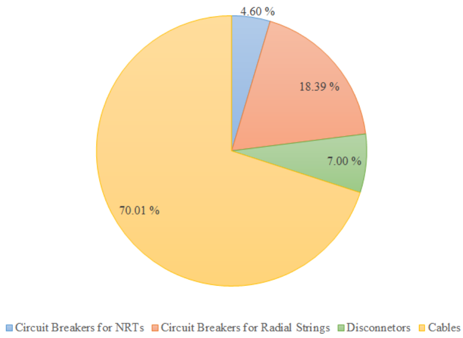

(a) Base Case

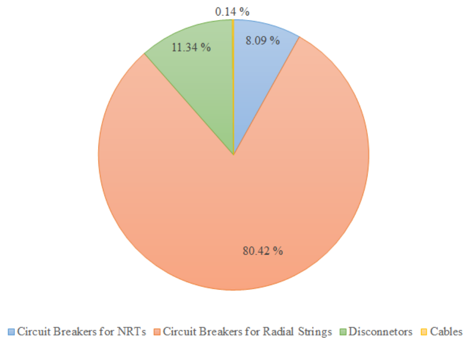

(b) Multi Ring

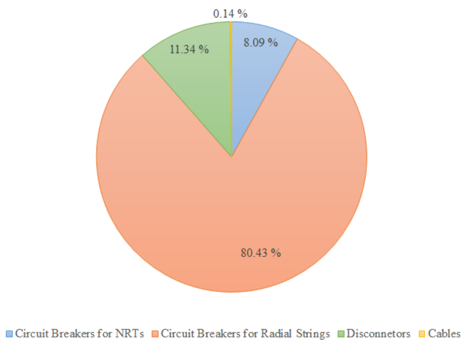

(c) Double Ring

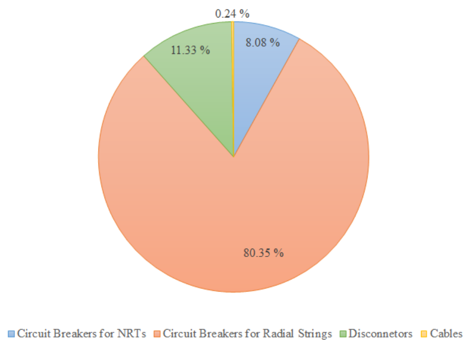

(d) Single Ring

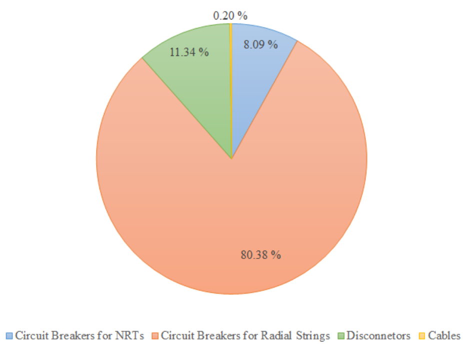

(e) Single Shared Ring

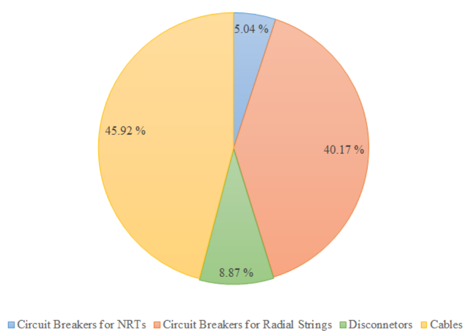

(f) Double Shared Half Ring

Figure 21: Components contribution to outage time for each configuration

9.5 Sensitivity Analysis

The reliability data for an offshore wind farm is highly uncertain as offshore wind farm grids rely on relatively new and advanced technology, and there are little quantitative data to be found for the failure statistics of them. This especially applies to offshore wind farms of the size analysed in this thesis, as they are only just now starting to construct wind farms of this size. The reliability data used in this thesis is a result of the work done by SINTEF and Kirkeby, but other sources uses different reliability inputs. Since the reliability data for the XLPE cable varies the most, a sensitivity analysis of this data is performed to see how it will influence the choice of configuration.

When changing either the frequency of failure for cables or the mean time to repair for the cable from 50 % of the inital value to 200 % of the inital value, the resulting changes are the same. The resulting total costs for each of the configurations are given in Figure 22 for a power production of 10 MW and in Figure 23 for the time varying power production. For both figures it can be seen that the multi ring configuration is the desirable one for all values of MTTR from 50 % to 200 % of the given value for the cables. It can also be seen that the cost of the base case decreases drastically with a decrease in MTTR. But the outage time for a cable has to be less than 500 hours to make the base case the more desirable one, which is not likely as it complicated to repair an offshore cable.

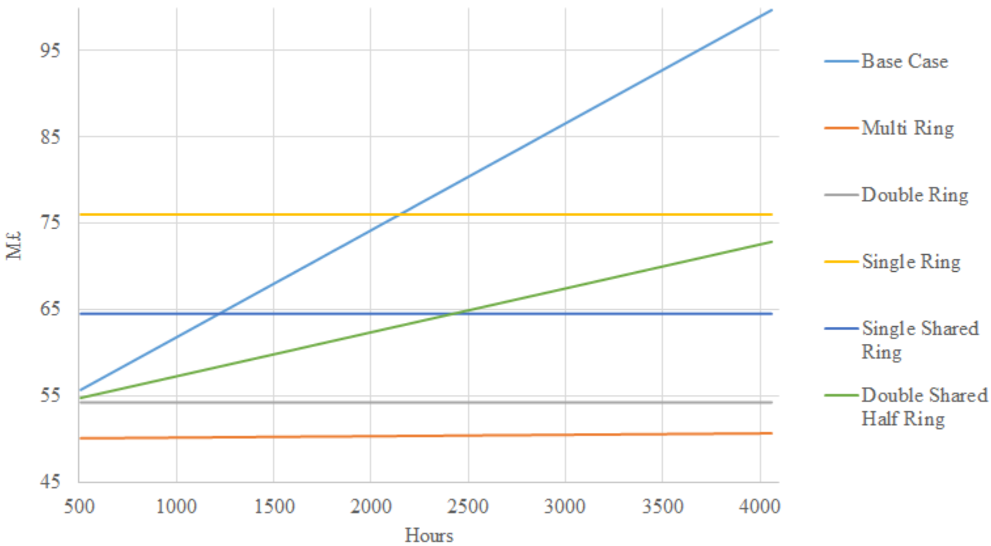

Figure 22: Resulting total costs as a function of change in MTTR for cables

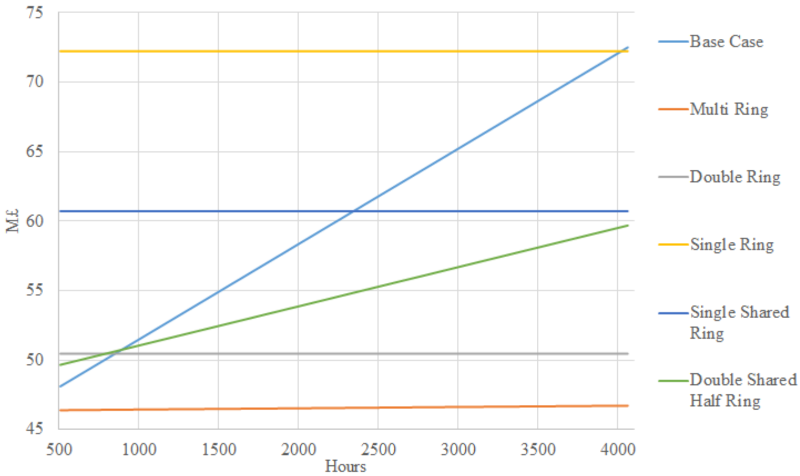

Figure 23: Resulting total costs as a function of change in MTTR for cables with Time Varying Production

In addition to the reliability data for the cables a sensitivity analysis is done on the costs of cables, as these contribute a lot to the total costs of a configurations. They are also likely to change some as the technology improves and the demand for offshore cables increases. The cable costs are analysed to change from 50 % of the initial value, to 200 % of the initial value. Figure 24 and 25 shows the resulting total costs for all configurations for 10MW production and time varying production, respectively. Both figures show that the multi ring configuration is the most profitable up to the point where the cable costs are at approximately 60 % of current costs. At this point the double ring configuration seems to be better. However, since the double ring configuration is designed with cables with too small cross-sections for this case, the multi ring configuration will probably still be more profitable as an increase in cross-section for the double ring will lead to an increase in cable costs.

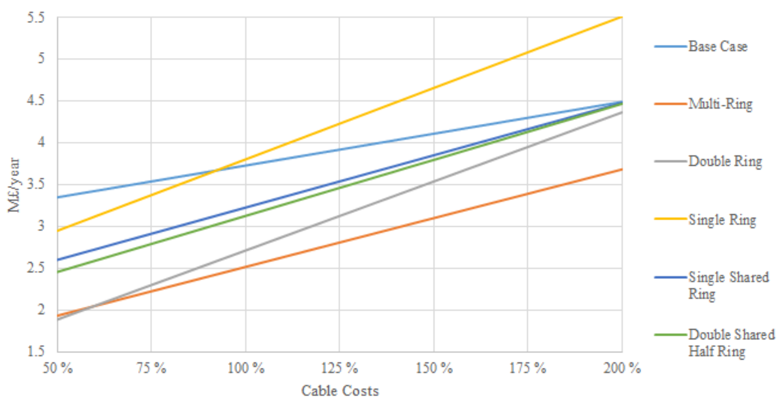

Figure 24: Resulting total annual costs as a function of change in cables costs

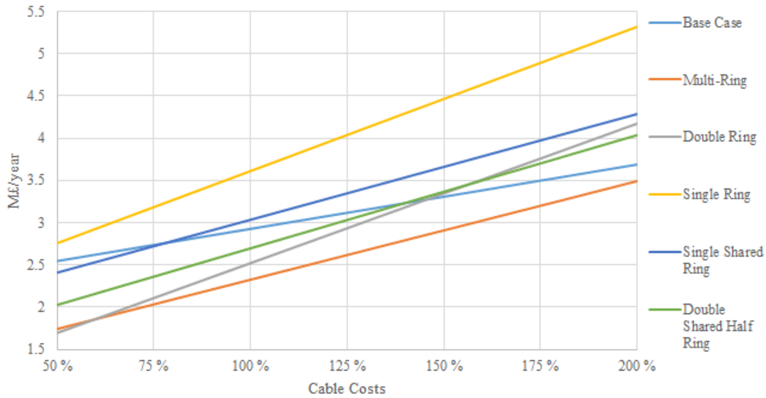

Figure 25: Resulting total annual costs as a function of change in cables costs with Time Varying Production

In "Optimal redundans i Dogger Bank referansevindpark" a similar analysis was performed as the one done in this thesis. There it was discovered that the power losses contribute a great deal to the lost energy in the DRW. As a result this was included in this thesis. The power loss varies depending on the resistance of the cable as well as the power flow through it. For the previous analysis a decision to use the lowest possible cross-section for the given power flow was done. In this section all the cables used in the base case, single ring and single shared ring configurations are converted to be the same as the cable with the biggest cross-section in the configuration, i.e. a cross section of 240 mm^2 for all cables. These three configurations are chosen as these have the highest costs of power loss. This alternation will increase the cable costs, which has also been included, and the total costs are shown in Figure 26 and 27.

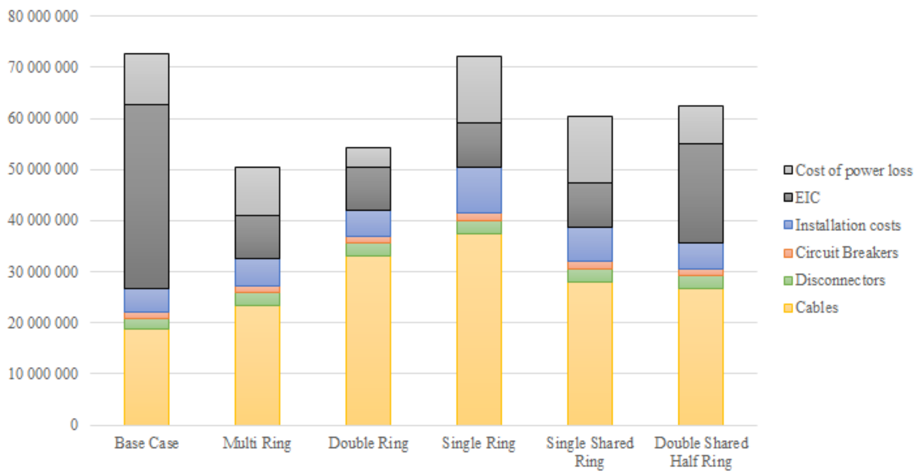

Figure 26: Costs for each configuration distributed by components

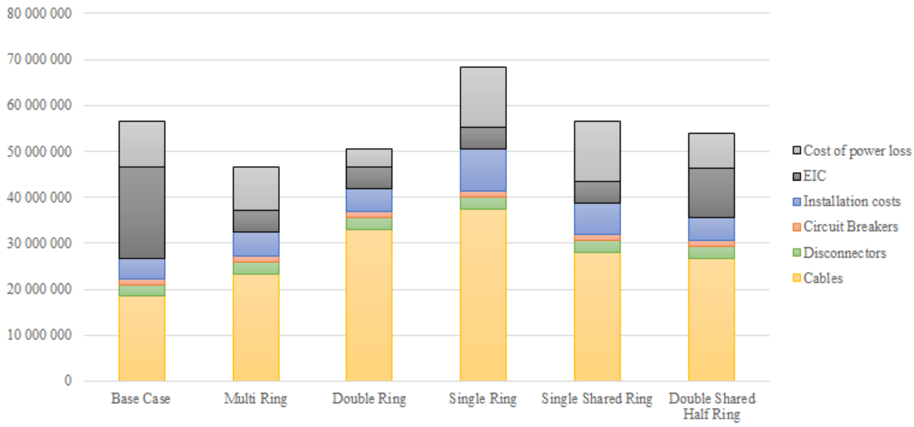

Figure 27: Costs for each configuration distributed by components with time varying production

Here the multi ring, double ring and double shared half ring contributions have the same cables as before as the power loss costs is a much smaller part of the total costs for these configurations. It can still be seen that the multi ring configuration is the most profitable one for both perspectives. For the case with time varying power production, the three changed configurations are still the most expensive ones, while the single shared ring configuration can be considered the third best alternative if a power production of 10 MW per turbine is assumed. The single ring configuration is the most expensive in most of the cases as this design uses ten times 7.2 km long redundancy cables which is quite expensive both in terms of cable costs and power losses.

Lastly, a sensitivity analysis is performed analysing if the number of years the wind farm is operational will change the outcome. Given new and better technology a lifetime of 30 years for an offshore wind farm is not unreasonable. However, the longevity of an offshore wind farm of this size is uncertain as they have only just began construction of them, and a lifetime down to 15 year has been assessed.

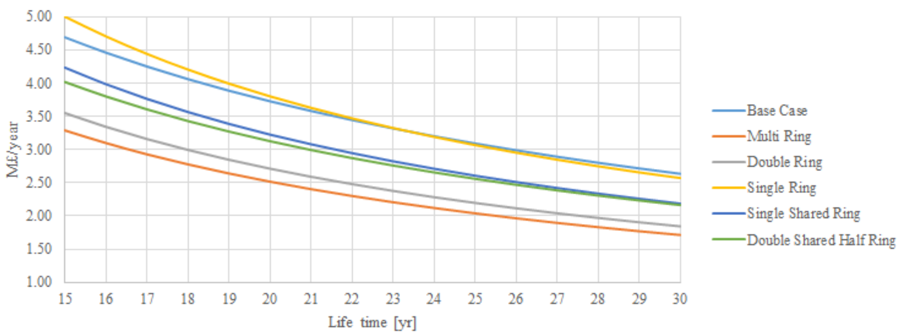

Figure 28: Costs per year for each configuration

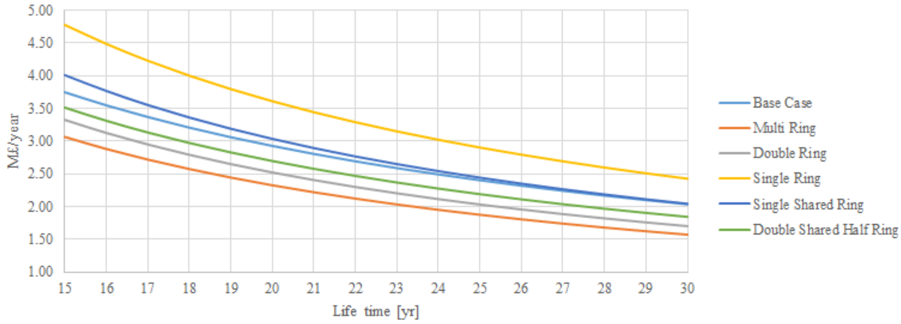

Figure 29: Costs per year for each components with time varying production

Figure 28 shows the costs per year for a production of 10 MW per turbine, while Figure 29 shows the same results for the time varying production. For all configurations the longer the lifte, the smaller the costs per year will be. Again, both figures suggests that the multi ring design is the optimum configuration for the Dogger Bank Reference Wind Farm.

10 Conclusion

The primary conclusion to this thesis is that a design of the multi ring configuration of the DRW is the best solution in terms of reliability and economy. For any sensitivity analysis performed, the multi ring configuration still seems to be the most profitable. It could be possible to find the point where the multi ring configuration is no longer the cheapest solution, but that would suggest using unrealistic values for the reliability data and the economic data. The next choice would be the double ring configuration with a redundancy level of 75 %, if a multi ring configuration for some reason was undesirable. It could therefore be said that a configuration that provides redundancy shared by more than one string is desirable. It is more expensive to use one long cable with small cross-section for redundancy than several short ones with larger cross-sections.

Of the components analysed in this thesis, the cables contribute the most to the reliability in the configurations without full redundancy. When including the redundancy cables they provide an alternate route for the power during fault in the main cables, and the reliability contribution is greatly reduced. The next great contributor to the reliability is then the circuit breakers located at the start of each string in the configurations.

The double ring configuration seems to be a viable alternative given a reduction of the costs of cables, however, since ABB does not yet provide 66 kV XLPE cables with large enough cross-sections to withstand the rated power, this was deprecated. During the sensitivity analysis, the multi ring configuration has been the optimum solution to the DRW, for all values. These values have been chosen to depict reality rather than finding the point where the multi ring configuration no longer presents as the best solution.

Throughout this thesis a comparison between the results for a production of 10 MW per wind turbine, and time varying production has been made. When analysing the costs of the wind farm, the actual expected wind energy production will determine how much one could expect to make, and how much is actually lost due to faults in the components. For this reason it would be most advantageous to choose a configuration based on the time varying production. In this thesis the results give the same conclusion, regardless of which production level is assumed, and that is the multi ring configuration with a level of 100 % redundancy. This differ from previous work done by Vingdal, which came to the conclusion of choosing multi ring configuration with 75 % redundancy. This might be caused by including the lost profit due to power losses in this thesis, which have not been included in “Optimal redundans i Dogger Bank referansevindpark”.

10.1 Further Works

A sensitivity analysis for a change in energy prices has not been performed as there have been legislation determining a fixed price for offshore wind energy some time ahead for the UK. This could however be of some interest, especially for other wind farms of the same size in other countries.

Another essential part in choosing the preferable configuration is ensuring that the system can withstand the requirements of security for an offshore wind farm. This can be done by performing more technical analyses such as a short circuit analysis to determine cross-sections of cables able to withstand short periods of time with very high current.

To carry forward with the conclusion of this thesis, it would be advantageous to perform a full reliability analysis including the components neglected in this thesis, such as turbines, transformers, 132kV cables, and control systems.

Lastly, a closer look at the assumptions made for the reliability analysis should be done. One cable has a mean time to repair of 2030 hours, is it reasonable to assume that no other fault will occur during this time? Especially at the beginning and end of the lifetime of the wind farm there occur more faults than in the middle of the lifetime. This might influence the reliability much more than can be neglected.

References

[1] ABB. *XLPE Submarine Cable Systems, Attachemnt to XLPE Land Cable Systems - User's Guide*. Brochure. Apr. 2010. URL: http://www04.abb.com/global/seitp/seitp202.nsf/0/badf833d6cb8d46dc1257c0b002b3702/$file/XLPE+Submarine+Cable+Systems+2GM5007+.pdf (visited on 05/04/2016).

[2] XLPE ABB. *Submarine Cable Systems: Attachment to XLPE Land Cable Systems - Users Guide*. 2010. URL: http://www04.abb.com/global/seitp/seitp202.nsf/0/badf833d6cb8d46dc1257c0b002b3702/$file/XLPE+Submarine+Cable+Systems+2GM5007+.pdf (visited on 03/03/2016).

[3] Todd Beatty. *AREVA Reference*. Letter. ALSTROM - Grid Products Circuit Breakers. Nov. 15, 2010. URL: http://www.ci.hercules.ca.us/documents/Agendas/Council/2010/11-23-10/Item%20VIII.A.1%20HMU%20Breakers%20Atch%204.pdf (visited on 05/27/2016).

[4] Department of Energy and Climate Change. *Electricity Market Reform: Delivering UK Investment*. June 2013. URL: https://www.gov.uk/government/uploads/system/uploads/attachment_data/file/209276/EMR_Spending_Review_Announcement_-_FINAL_PDF.pdf (visited on 06/09/2016).

[5] Harald Fien. *High-Voltage Circuit-Breakers: Trends and Recent Developments*. 2011. URL: http://www.energy.siemens.com/nl/pool/hq/power-transmission/high-voltage-products/circuit-breaker/trends_en.pdf (visited on 06/10/2016).

[6] Forewind. *Forewind - Dogger Bank Creyke Beck*. 2011–2016. URL: http://www.forewind.co.uk/projects/dogger-bank-creyke-beck.html (visited on 03/25/2016).

[7] Douglas C Giancoli. "25. Electric Currencts and Resistance". In: *Physics for scientists & engineers with modern physics*. 4th. Upper Saddle River, N.J.: Pearson Prentice Hall, 2009. ISBN: 978-0-13-149508-1 978-0-13-157849-4.

[8] 60287 IEC. *Electric Cables - Calculation of the Current Rating - Part 1-1: Current rating equations (100% load factor) and calculation of losses - General International Electrotechnical Commission*. Dec. 1, 2014.

[9] IEEE Power & Energy Society et al. *IEEE guide for electric power distribution reliability indices*. OCLC: 808375932. New York: Institute of Electrical and Electronics Engineers, 2012. ISBN: 978-0-7381-7275-0. URL: http://ieeexplore.ieee.org/servlet/opac?punumber=6209379 (visited on 05/30/2016).

[10] Henrik Kirkeby. *NOWITECH Reference Wind Farm Electrical Design*. Mar. 26, 2014.

[11] Henrik Kirkeby and K. Merz. *Layout and Electrical Design of a 1.2 GW Wind Farm for Research on the Next Generation of Offshore Wind Energy Technologies*. Trondheim. 2014.

[12] Henrik Kirkeby and John Olav Tande. "The NOWITECH Reference Wind Farm". In: *Energy Procedia* 53 (2014), pp. 300–312. ISSN: 18766102. DOI: 10.1016/j.egypro.2014.07.239. URL: http://linkinghub.elsevier.com/retrieve/pii/S1876610214011163 (visited on 02/10/2016).

[13] G. Kjolle and K. Sand. "RELRAD-an analytical approach for distribution system reliability assessment". In: *Transmission and Distribution Conference, 1991., Proceedings of the 1991 IEEE Power Engineering Society*. Transmission and Distribution Conference, 1991., Proceedings of the 1991 IEEE Power Engineering Society. Sept. 1991, pp. 729–734. DOI: 10.1109/TDC.1991.169586.

[14] Jan Machowski, Janusz W. Bialek, and J. R. Bumby. *Power system dynamics: stability and control*. 2nd ed. Chichester, U.K: Wiley, 2008. 629 pp. ISBN: 978-0-470-72558-0.

[15] Karl O. Merz. *Dogger Bank Reference Wind Power Plant: Layout, Electrical Design, and Wind Turbine Specification*. Jan. 21, 2016. URL: `https://www.sintef.no/globalassets/project/eera-deepwind2016/presentations/x2_merz.pdf` (visited on 06/01/2016).

[16] Nicola Barberis Negra. "Offshore Wind Power: Grid Connection and Reliability". Denmark: Aalborg University, 2008. 259 pp.

[17] Erika Nord. "Cost Estimation of Wind Farms' Internal Grids". Stockholm: KTH Royal Institue of Technology, 2011. URL: `https://www.diva-portal.org/smash/get/diva2:456427/FULLTEXT01.pdf` (visited on 05/16/2016).

[18] Shuangwen (Shawn) Sheng. "Report on Wind Turbine Subsystem Reliability - A Survey of Various Databases". NREL - National Renewable Energy Laboratory. June 2013. URL: `http://www.nrel.gov/docs/fy13osti/59111.pdf` (visited on 06/07/2016).

[19] J. S. Shin et al. "Reliability evaluation considering structures of a large scale wind farm". In: *2013 15th European Conference on Power Electronics and Applications (EPE)*. 2013 15th European Conference on Power Electronics and Applications (EPE). Sept. 2013, pp. 1–10. DOI: `10.1109/EPE.2013.6634750`.

[20] Service Management Siemens AG. *High Voltage Disconnectors and Earthing Switches*. Nov. 2014. URL: `http://www.energy.siemens.com/us/pool/hq/power-transmission/high-voltage-products/disconnectors/downloads/high-voltage-disconnectors-and-earthing-switches_EN.PDF` (visited on 05/28/2016).

[21] Energy Research SINTEF. *Empirical Data*. Trondheim, 2015.

[22] New Zealand Transpower. *ACS Disconnectors and Earth Switches*. Nov. 15, 2013. URL: `https://www.transpower.co.nz/sites/default/files/uncontrolled_docs/PD19%20-%20POD%20-%20ACS%20Disconnectors%20and%20Earth%20Switches.pdf` (visited on 05/27/2016).

[23] Kjetil Uhlen. "Voltage Balance and Power Flow". Subject TET4115. NTNU, 25.08.14. URL: `https://files.itslearning.com/` (visited on 04/28/2016).

[24] Vijay Venu Vadlamudi. "Interruption Costs - Reliability Assessment". Subject ELK 10. NTNU, 6.11.15. URL: `https://files.itslearning.com` (visited on 04/28/2016).

[25] Vijay Venu Vadlamudi. "Reliability Assessment of Power Systems -Introduction". Subject ELK 10. NTNU, 23.10.15. URL: `https://files.itslearning.com` (visited on 04/28/2016).

[26] Vijay Venu Vadlamudi. "RELRAD Methodology For Distribution System Reliability". Subject ELK 10. NTNU, 23.10.15.

[27] Hanne Merete Vefsnmo and Henrik Kirkeby. *Reliability Study of Dudgeon Offshore Wind Farm*. Trondheim: SINTEF Energy Research, June 18, 2014, p. 36.

[28] Kari Vingdal. "Optimal redundans i Dogger Bank referansevindpark". Prosjektoppgave. Trondheim: NTNU, 2014. 60 pp.

[29] Kari Vingdal. "Optimal redundans i Dogger Bank referansevindpark". Master. Trondheim: NTNU, 2015. 126 pp.

[30] Dong Wind. *A History of Offshore Wind Power*. 2015. URL: `http://offshorewind.works/inform/a-history-of-offshore-wind-power/` (visited on 04/27/2016).

[31] EUR to GPB XE. *XE: (EUR/GBP) Euro to British Pound Rate*. 2016. URL: `http://www.xe.com/currencyconverter/convert/?Amount=1&From=EUR&To=GBP` (visited on 05/28/2016).
[32] USD to GBP XE. *XE: (USD/GBP) US Dollar to British Pound Rate*. 2016. URL: `http://www.xe.com/currencyconverter/convert/?Amount=1&From=USD&To=GBP` (visited on 05/28/2016).
[33] Ray D. Zimmerman and Carlos E. Murillo-Sánchez. *MatPower 5.1 User's Manual*. 20.03.15. URL: `http://www.pserc.cornell.edu/matpower/manual.pdf` (visited on 04/29/2016).

A Configurations

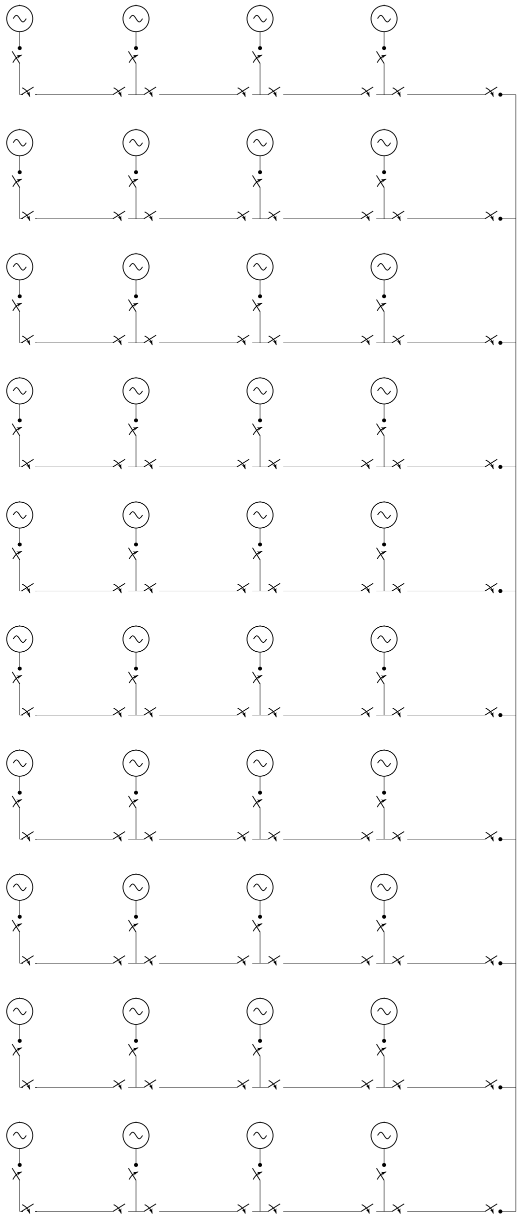

Figure 30: Configuration of the base case

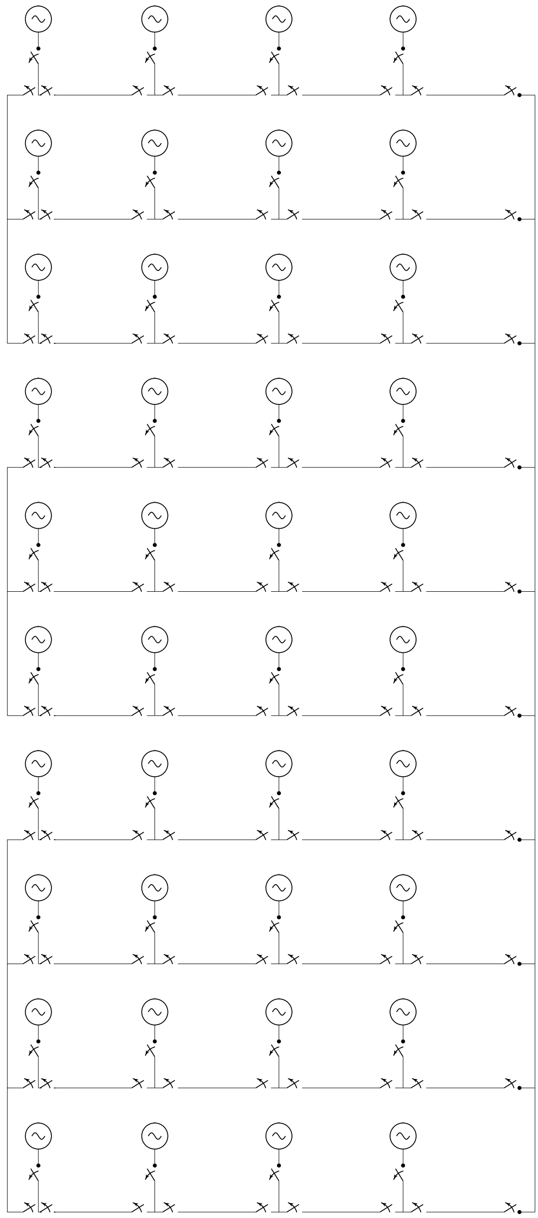

Figure 31: Multi-ring Configuration

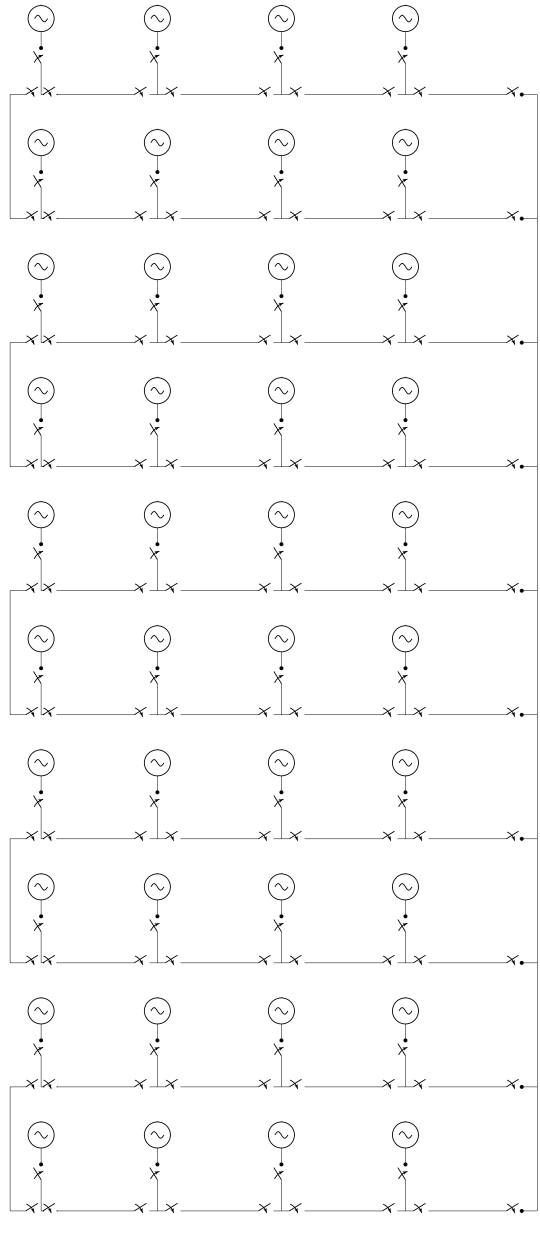

Figure 32: Double Ring Configuration

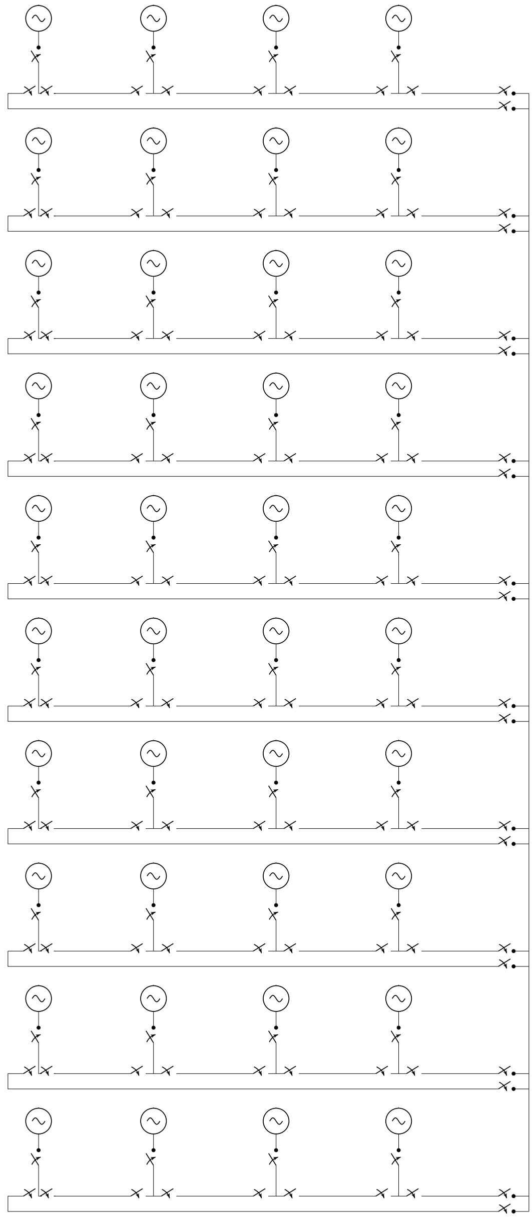

Figure 33: Single Ring Configuration

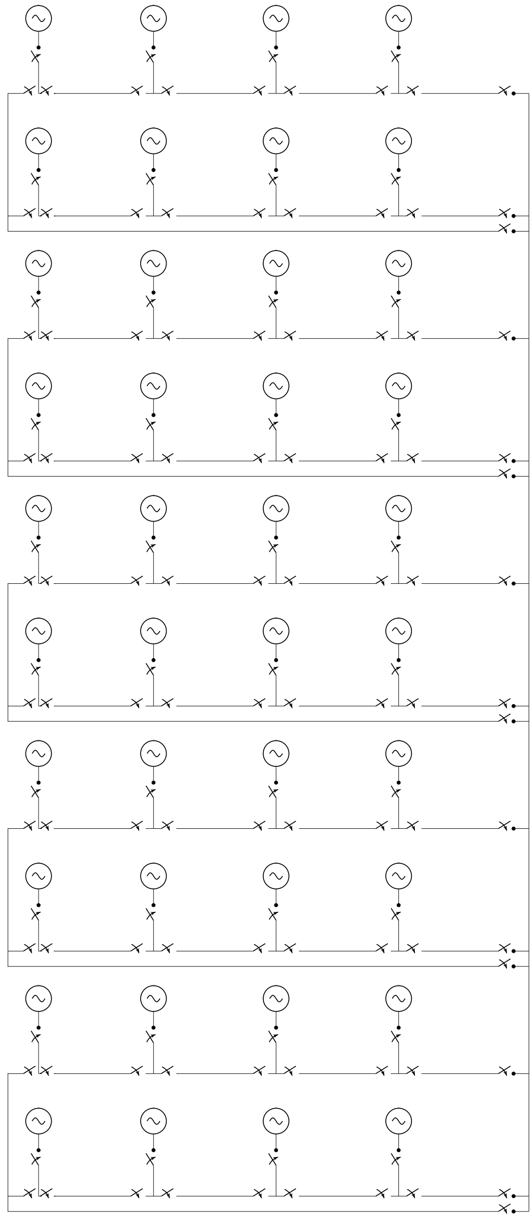

Figure 34: Single Shared Ring Configuration

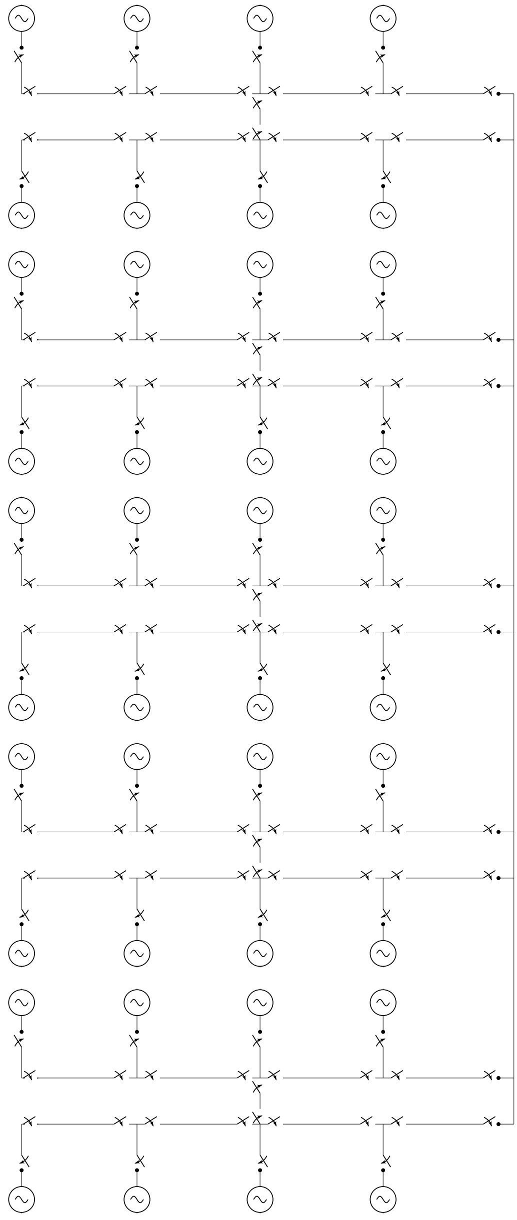

Figure 35: Double Shared Half-Ring Configuration

B Redundancy

Table 14: Cable selection for multi-ring 3-string section

Lvl.of red.	P_i [MW]	P_{red} [MW]	P_{tot} [MW]	I_n [A]	$I_{n,ABB}$ [A]	Cross Section [mm^2]	Length of Cables [km]	C_{cable} [M£/km]	Total Cable Costs [M£]
1	40	20	60	656	715	630	5.4	0.408697	2.206962
	30	20	50	547	590	400	5.4	0.318885	1.721977
	20	20	40	437	480	240	5.4	0.259553	1.401587
	10	20	30	328	340	120	5.4	0.203739	1.100191
	0	40	40	437	480	240	3.6	0.259553	0.934391
0.9	40	18	58	634	655	500	5.4	0.362178	1.955760
	30	18	48	525	530	300	5.4	0.284564	1.536648
	20	18	38	416	420	185	5.4	0.233292	1.259775
	10	18	28	306	340	120	5.4	0.203739	1.100191
	0	36	36	394	420	185	3.6	0.233292	0.839850
0.8	40	16	56	612	655	500	5.4	0.362178	1.955760
	30	16	46	503	530	300	5.4	0.284564	1.536648
	20	16	36	394	420	185	5.4	0.233292	1.259775
	10	16	26	284	300	95	5.4	0.190985	1.031319
	0	32	32	350	375	150	3.6	0.215964	0.777470
0.7	40	14	54	591	655	500	5.4	0.362178	1.955760
	30	14	44	481	530	300	5.4	0.284564	1.536648
	20	14	34	372	375	150	5.4	0.215964	1.166205
	10	14	24	262	300	95	5.4	0.190985	1.031319
	0	28	28	306	340	120	3.6	0.203739	0.733461
0.6	40	12	52	569	590	400	5.4	0.318885	1.721977
	30	12	42	459	480	240	5.4	0.259553	1.401587
	20	12	32	350	375	150	5.4	0.215964	1.166205
	10	12	22	241	300	95	5.4	0.190985	1.031319
	0	24	24	262	300	95	3.6	0.190985	0.687546
0.5	40	10	50	547	590	400	5.4	0.318885	1.721977
	30	10	40	437	480	240	5.4	0.259553	1.401587
	20	10	30	328	340	120	5.4	0.203739	1.100191
	10	10	20	219	300	95	5.4	0.190985	1.031319
	0	20	20	219	300	95	3.6	0.190985	0.687546

Table 15: Cable selection for multi-ring 4-string section

Lvl.of red.	P_i [MW]	P_{red} [MW]	P_{tot} [MW]	I_n [A]	$I_{n,ABB}$ [A]	Cross Section [mm^2]	Length of Cables [km]	C_{cable} [M£/km]	Total Cable Costs [M£]
1	40	13.33	53.33	583	590	400	7.2	0.318885	2.295969
	30	13.33	43.33	474	480	240	7.2	0.259553	1.868782
	20	13.33	33.33	365	375	150	7.2	0.215964	1.554941
	10	20	30	328	340	120	7.2	0.203739	1.466922
	0	40	40	437	480	240	5.4	0.259553	1.401587
0.9	40	12	52	569	590	400	7.2	0.318885	2.295969
	30	12	42	459	480	240	7.2	0.259553	1.868782
	20	12	32	350	375	150	7.2	0.215964	1.554941
	10	17	27	295	300	95	7.2	0.190985	1.375092
	0	36	36	394	420	185	5.4	0.233292	1.259775
0.8	40	10.67	50.67	554	590	400	7.2	0.318885	2.295969
	30	10.67	40.67	445	480	240	7.2	0.259553	1.868782
	20	10.67	30.67	335	340	120	7.2	0.203739	1.466922
	10	14	24	262	300	95	7.2	0.190985	1.375092
	0	32	32	350	375	150	5.4	0.215964	1.166205
0.7	40	9.33	49.33	539	590	400	7.2	0.318885	2.295969
	30	9.33	39.33	430	480	240	7.2	0.259553	1.868782
	20	9.33	29.33	321	340	120	7.2	0.203739	1.466922
	10	11	21	230	300	95	7.2	0.190985	1.375092
	0	28	28	306	340	120	5.4	0.203739	1.100191
0.6	40	8	48	525	530	300	7.2	0.284564	2.048863
	30	8	38	416	420	185	7.2	0.233292	1.679699
	20	8	28	306	340	120	7.2	0.203739	1.466922
	10	8	18	197	300	95	7.2	0.190985	1.375092
	0	24	24	262	300	95	5.4	0.190985	1.031319
0.5	40	6.67	46.67	510	530	300	7.2	0.284564	2.048863
	30	6.67	36.67	401	420	185	7.2	0.233292	1.679699
	20	6.67	26.67	292	300	95	7.2	0.190985	1.375092
	10	6.67	16.67	182	300	95	7.2	0.190985	1.375092
	0	20	20	219	300	95	5.4	0.190985	1.031319

Table 16: Cable selection for double ring

Lvl.of red.	P_i [MW]	P_{red} [MW]	P_{tot} [MW]	I_n [A]	$I_{n,ABB}$ [A]	Cross Section [mm^2]	Length of Cables [km]	C_{cable} [M£/km]	Total Cable Costs [M£]
1	40	40	80	875	825	1000	3.6	0.513795	1.849661
	30	40	70	766	825	1000	3.6	0.513795	1.849661
	20	40	60	656	715	630	3.6	0.408697	1.471308
	10	40	50	547	590	400	3.6	0.318885	1.147984
	0	40	40	437	480	240	1.8	0.259553	0.467196
0.9	40	36	76	831	825	1000	3.6	0.513795	1.849661
	30	36	66	722	775	800	3.6	0.462527	1.665098
	20	36	56	612	655	500	3.6	0.362178	1.303840
	10	36	46	503	530	300	3.6	0.284564	1.024432
	0	36	36	394	420	185	1.8	0.233292	0.419925
0.8	40	32	72	787	825	1000	3.6	0.513795	1.849661
	30	32	62	678	715	630	3.6	0.408697	1.471308
	20	32	52	569	590	400	3.6	0.318885	1.147984
	10	32	42	459	480	240	3.6	0.259553	0.934391
	0	32	32	350	375	150	1.8	0.215964	0.388735
0.7	40	28	68	744	775	800	3.6	0.462527	1.665098
	30	28	58	634	655	500	3.6	0.362178	1.303840
	20	28	48	525	530	300	3.6	0.284564	1.024432
	10	28	38	416	420	185	3.6	0.233292	0.839850
	0	28	28	306	340	120	1.8	0.203739	0.366730
0.6	40	24	64	700	715	630	3.6	0.408697	1.471308
	30	24	54	591	655	500	3.6	0.362178	1.303840
	20	24	44	481	530	300	3.6	0.284564	1.024432
	10	24	34	372	375	150	3.6	0.215964	0.777470
	0	24	24	262	300	95	1.8	0.190985	0.343773
0.5	40	20	60	656	715	630	3.6	0.408697	1.471308
	30	20	50	547	590	400	3.6	0.318885	1.147984
	20	20	40	437	480	240	3.6	0.259553	0.934391
	10	20	30	328	340	120	3.6	0.203739	0.733461
	0	20	20	219	300	95	1.8	0.190985	0.343773

Table 17: Cable selection for Single Ring

Lvl.of red.	P_i [MW]	P_{red} [MW]	P_{tot} [MW]	I_n [A]	$I_{n,ABB}$ [A]	Cross Section [mm^2]	Length of Cables [km]	C_{cable} [M£/km]	Total Cable Costs [M£]
1	40		40	437	480	240	1.8	0.259553	0.467196
	30		30	328	340	120	1.8	0.203739	0.366730
	20		20	219	300	95	1.8	0.190985	0.343773
	10	20	30	328	340	120	1.8	0.203739	0.366730
	0	40	40	437	480	240	7.2	0.259553	1.868782
0.9	40		40	437	480	240	1.8	0.259553	0.467196
	30		30	328	340	120	1.8	0.203739	0.366730
	20		20	219	300	95	1.8	0.190985	0.343773
	10	17	27	295	340	120	1.8	0.203739	0.366730
	0	36	36	394	420	185	7.2	0.233292	1.679699
0.8	40		40	437	480	240	1.8	0.259553	0.467196
	30		30	328	340	120	1.8	0.203739	0.366730
	20		20	219	300	95	1.8	0.190985	0.343773
	10	14	24	262	300	95	1.8	0.190985	0.343773
	0	32	32	350	375	150	7.2	0.215964	1.554941
0.7	40		40	437	480	240	1.8	0.259553	0.467196
	30		30	328	340	120	1.8	0.203739	0.366730
	20		20	219	300	95	1.8	0.190985	0.343773
	10	11	21	230	300	95	1.8	0.190985	0.343773
	0	28	28	306	340	120	7.2	0.203739	1.466922
0.6	40		40	437	480	240	1.8	0.259553	0.467196
	30		30	328	340	120	1.8	0.203739	0.366730
	20		20	219	300	95	1.8	0.190985	0.343773
	10	8	18	197	300	95	1.8	0.190985	0.343773
	0	24	24	262	300	95	7.2	0.190985	1.375092
0.5	40		40	437	480	240	1.8	0.259553	0.467196
	30		30	328	340	120	1.8	0.203739	0.366730
	20		20	219	300	95	1.8	0.190985	0.343773
	10	5	15	164	300	95	1.8	0.190985	0.343773
	0	20	20	219	300	95	7.2	0.190985	1.375092

Table 18: Cable selection for Single Shared Ring

Lvl.of red.	P_i [MW]	P_{red} [MW]	P_{tot} [MW]	I_n [A]	$I_{n,ABB}$ [A]	Cross Section $[mm^2]$	Length of Cables [km]	C_{cable} [M£/km]	Total Cable Costs [M£]
1	40		40	437	480	240	3.6	0.259553	0.934391
	30		30	328	340	120	3.6	0.203739	0.733461
	20		20	219	300	95	3.6	0.190985	0.687546
	10	20	30	328	340	120	3.6	0.203739	0.733461
	0	40	40	437	480	240	9	0.259553	2.335978
0.9	40		40	437	480	240	3.6	0.259553	0.934391
	30		30	328	340	120	3.6	0.203739	0.733461
	20		20	219	300	95	3.6	0.190985	0.687546
	10	17	27	295	300	95	3.6	0.190985	0.687546
	0	36	36	394	420	185	9	0.233292	2.099624
0.8	40		40	437	480	240	3.6	0.259553	0.934391
	30		30	328	340	120	3.6	0.203739	0.733461
	20		20	219	300	95	3.6	0.190985	0.687546
	10	14	24	262	300	95	3.6	0.190985	0.687546
	0	32	32	350	375	150	9	0.215964	1.943676
0.7	40		40	437	480	240	3.6	0.259553	0.934391
	30		30	328	340	120	3.6	0.203739	0.733461
	20		20	219	300	95	3.6	0.190985	0.687546
	10	11	21	230	300	95	3.6	0.190985	0.687546
	0	28	28	306	340	120	9	0.203739	1.833652
0.6	40		40	437	480	240	3.6	0.259553	0.934391
	30		30	328	340	120	3.6	0.203739	0.733461
	20		20	219	300	95	3.6	0.190985	0.687546
	10	8	18	197	300	95	3.6	0.190985	0.687546
	0	24	24	262	300	95	9	0.190985	1.718865
0.5	40		40	437	480	240	3.6	0.259553	0.934391
	30		30	328	340	120	3.6	0.203739	0.733461
	20		20	219	300	95	3.6	0.190985	0.687546
	10	5	15	164	300	95	3.6	0.190985	0.687546
	0	20	20	219	300	95	9	0.190985	1.718865

Table 19: Cable Selection for Double Shared Half-Ring

Lvl.of red.	P_i [MW]	P_{red} [MW]	P_{tot} [MW]	I_n [A]	$I_{n,ABB}$ [A]	Cross Section [mm^2]	Length of Cables [km]	C_{cable} [M£/km]	Total Cable Costs [M£]
1	40	40	80	875	825	1000	3.6	0.513795	1.849661
	30	40	70	766	775	800	3.6	0.462527	1.665098
	20		20	219	300	95	3.6	0.190985	0.687546
	10		10	109	300	95	3.6	0.190985	0.687546
	0	40	40	437	480	240	1.8	0.259553	0.467196
0.9	40	36	76	831	825	1000	3.6	0.513795	1.849661
	30	36	66	722	775	800	3.6	0.462527	1.665098
	20		20	219	300	95	3.6	0.190985	0.687546
	10		10	109	300	95	3.6	0.190985	0.687546
	0	36	36	394	420	185	1.8	0.233292	0.419925
0.8	40	32	72	787	825	1000	3.6	0.513795	1.849661
	30	32	62	678	715	630	3.6	0.408697	1.471308
	20		20	219	300	95	3.6	0.190985	0.687546
	10		10	109	300	95	3.6	0.190985	0.687546
	0	32	32	350	375	150	1.8	0.215964	0.388735
0.7	40	28	68	744	775	800	3.6	0.462527	1.665098
	30	28	58	634	655	500	3.6	0.362178	1.303840
	20		20	219	300	95	3.6	0.190985	0.687546
	10		10	109	300	95	3.6	0.190985	0.687546
	0	28	28	306	340	120	1.8	0.203739	0.366730
0.6	40	24	64	700	715	630	3.6	0.408697	1.471308
	30	24	54	591	655	500	3.6	0.362178	1.303840
	20		20	219	300	95	3.6	0.190985	0.687546
	10		10	109	300	95	3.6	0.190985	0.687546
	0	24	24	262	300	95	1.8	0.190985	0.343773
0.5	40	20	60	656	715	630	3.6	0.408697	1.471308
	30	20	50	547	590	400	3.6	0.318885	1.147984
	20		20	219	300	95	3.6	0.190985	0.687546
	10		10	109	300	95	3.6	0.190985	0.687546
	0	20	20	219	300	95	1.8	0.190985	0.343773

C Cable Specifications

Table 20: Three-core cables with lead sheath, nominal voltage 66kV[2]

Cross-section of conductor $[mm^2]$	Capacitance $[\mu F/km]$	Inductance $[mH/km]$	I_n Copper conductor [A]
95	0.17	0.44	300
120	0.18	0.43	340
150	0.19	0.41	375
185	0.20	0.40	420
240	0.22	0.38	480
300	0.24	0.37	530
400	0.26	0.35	590
500	0.29	0.34	655
630	0.32	0.33	715
800	0.35	0.32	775
1000	0.38	0.31	825

Table 20 shows tha data given in Table 33 and Table 45 in *Submarine Cable Systems: Attachment to XLPE Land Cable Systems - Users Guide.*

Table 21: Calculated Cable Data Implemented in MATPOWER

Cross-sec.	R_{AC}	X_L	B_C	R_{pu}	X_{pu}	B_{pu}
95	0.3578947	0.1382301	0.0000534	0.0328645	0.0126933	0.0005816
120	0.2833333	0.1350885	0.0000565	0.0260178	0.0124048	0.0006158
150	0.2266667	0.1288053	0.0000597	0.0208142	0.0118279	0.0006500
185	0.1837838	0.1256637	0.0000628	0.0168764	0.0115394	0.0006842
240	0.1416667	0.1193805	0.0000691	0.0130089	0.0109624	0.0007527
300	0.1133333	0.1162389	0.0000754	0.0104071	0.0106739	0.0008211
400	0.0850000	0.1099557	0.0000817	0.0078053	0.0100969	0.0008895
500	0.0680000	0.1068142	0.0000911	0.0062443	0.0098085	0.0009921
630	0.0539683	0.1036726	0.0001005	0.0049558	0.0095200	0.0010948
800	0.0425000	0.1005310	0.0001100	0.0039027	0.0092315	0.0011974
1000	0.0340000	0.0973894	0.0001194	0.0031221	0.0089430	0.0013001

D MATPOWER code

```
function mpc = basecase
%   Power flow data for modified 11 bus, 40 gen case (based on PJM 5-bus
%   system)
%   Please see CASEFORMAT for details on the case file format.
%
%   (Based on data from ...
%     F.Li and R.Bo, "Small Test Systems for Power System Economic Studies",
%     Proceedings of the 2010 IEEE Power & Energy Society General Meeting
%
%   Created by Rui Bo in 2006, modified in 2010, 2014.
%   Distributed with permission.)
%
%   Based on data from Dogger Bank Reference Wind Farm
%
%   MATPOWER
%   $Id: case5.m 2408 2014-10-22 20:41:33Z ray $

%% MATPOWER Case Format : Version 2
mpc.version = '2';
%%-----  Power Flow Data  -----%%
%% system MVA base
mpc.baseMVA = 400;
%% bus data
% bus_i type  Pd  Qd  Gs  Bs  area  Vm  Va  baseKV  zone  Vmax    Vmin
mpc.bus = [
  1       1       400 0 0 0 1       1 0       66      1       1.1     0.9;
  2       2       0 0 0 0 1       1 0       66      1       1.1     0.9;
  3       2       0 0 0 0 1       1 0     66      1       1.1     0.9;
  4       2       0 0 0 0 1       1 0     66      1       1.1     0.9;
  5       2       0 0 0 0 1       1 0     66      1       1.1     0.9;
    6       2       0 0 0 0 1       1 0     66      1       1.1     0.9;
    7       2       0 0 0 0 1       1 0     66      1       1.1     0.9;
    8       2       0 0 0 0 1       1   0     66      1       1.1     0.9;
    9       2       0 0 0 0 1       1 0     66      1       1.1     0.9;
    10      2       0 0 0 0 1       1 0     66      1       1.1     0.9;
    11      2       0 0 0 0 1       1 0     66      1       1.1     0.9;
    12      2       0 0 0 0 1       1 0     66      1       1.1     0.9;
    13      2       0 0 0 0 1       1 0     66      1       1.1     0.9;
    14      2       0 0 0 0 1       1 0     66      1       1.1     0.9;
    15      2       0 0 0 0 1       1 0     66      1       1.1     0.9;
    16      2       0 0 0 0 1       1 0     66      1       1.1     0.9;
    17      2       0 0 0 0 1       1 0     66      1       1.1     0.9;
    18      2       0 0 0 0 1       1 0     66      1       1.1     0.9;
    19      2       0 0 0 0 1       1 0     66      1       1.1     0.9;
    20      2       0 0 0 0 1       1 0     66      1       1.1     0.9;
    21      2       0 0 0 0 1       1 0     66      1       1.1     0.9;
    22      2       0 0 0 0 1       1 0     66      1       1.1     0.9;
    23      2       0 0 0 0 1       1 0     66      1       1.1     0.9;
    24      2       0 0 0 0 1       1 0     66      1       1.1     0.9;
    25      2       0 0 0 0 1       1 0     66      1       1.1     0.9;
    26      2       0 0 0 0 1       1 0     66      1       1.1     0.9;
    27      2       0 0 0 0 1       1 0     66      1       1.1     0.9;
    28      2       0 0 0 0 1       1 0     66      1       1.1     0.9;
    29      2       0 0 0 0 1       1 0     66      1       1.1     0.9;
    30      2       0 0 0 0 1       1 0     66      1       1.1     0.9;
```

```
    31        2         0  0  0  0  1          1  0       66        1         1.1       0.9;
    32        2         0  0  0  0  1          1  0       66        1         1.1       0.9;
    33        2         0  0  0  0  1          1  0       66        1         1.1       0.9;
    34        2         0  0  0  0  1          1  0       66        1         1.1       0.9;
    35        2         0  0  0  0  1          1  0       66        1         1.1       0.9;
    36        2         0  0  0  0  1          1  0       66        1         1.1       0.9;
    37        2         0  0  0  0  1          1  0       66        1         1.1       0.9;
    38        2         0  0  0  0  1          1  0       66        1         1.1       0.9;
    39        2         0  0  0  0  1          1  0       66        1         1.1       0.9;
    40        2         0  0  0  0  1          1  0       66        1         1.1       0.9;
    41        2         0  0  0  0  1          1  0       66        1         1.1       0.9;
];

%% generator data
% bus Pg   Qg   Qmax   Qmin   Vg   mBase status   Pmax   Pmin   Pc1  Pc2  Qc1min   ...
    Qc1max   Qc2min   Qc2max   ramp_agc   ramp_10  ramp_30  ramp_q   apf
mpc.gen = [
  2  10   0  300       -300      1       400       1         10             0         0  0      ...
     0          0          0          0          0              0          0          0  ...
              0;
  3  10   0  300       -300      1       400       1         10             0         0  0      ...
     0          0          0          0          0              0          0          0  ...
              0;
  4  10   0  300       -300      1       400       1         10             0         0  0      ...
     0          0          0          0          0              0          0          0  ...
              0;
  5  10   0  300       -300      1       400       1         10             0         0  0      ...
     0          0          0          0          0              0          0          0  ...
              0;
    6  10   0  300       -300      1       400       1         10             0         0  0  ...
          0          0          0          0          0              0          0          0  ...
              0;
    7  10   0  300       -300      1       400       1         10             0         0  0  ...
          0          0          0          0          0              0          0          0  ...
              0;
    8  10   0  300       -300      1       400       1         10             0         0  0  ...
          0          0          0          0          0              0          0          0  ...
              0;
    9  10   0  300       -300      1       400       1         10             0         0  0  ...
          0          0          0          0          0              0          0          0  ...
              0;
    10    10   0  300       -300      1       400       1         10             0         0  ...
          0    0          0          0          0          0              0          0     ...
          0          0;
    11    10   0  300       -300      1       400       1         10             0         0  ...
          0    0          0          0          0          0              0          0     ...
          0          0;
    12    10   0  300       -300      1       400       1         10             0         0  ...
          0    0          0          0          0          0              0          0     ...
          0          0;
    13    10   0  300       -300      1       400       1         10             0         0  ...
          0    0          0          0          0          0              0          0     ...
          0          0;
    14    10   0  300       -300      1       400       1         10             0         0  ...
          0    0          0          0          0          0              0          0     ...
          0          0;
    15    10   0  300       -300      1       400       1         10             0         0  ...
          0    0          0          0          0          0              0          0     ...
          0          0;
```

```
16  10  0  300  -300  1  400  1  10  0  0 ...
    0   0  0    0     0  0    0  0 ...
    0   0;
17  10  0  300  -300  1  400  1  10  0  0 ...
    0   0  0    0     0  0    0  0 ...
    0   0;
18  10  0  300  -300  1  400  1  10  0  0 ...
    0   0  0    0     0  0    0  0 ...
    0   0;
19  10  0  300  -300  1  400  1  10  0  0 ...
    0   0  0    0     0  0    0  0 ...
    0   0;
20  10  0  300  -300  1  400  1  10  0  0 ...
    0   0  0    0     0  0    0  0 ...
    0   0;
21  10  0  300  -300  1  400  1  10  0  0 ...
    0   0  0    0     0  0    0  0 ...
    0   0;
22  10  0  300  -300  1  400  1  10  0  0 ...
    0   0  0    0     0  0    0  0 ...
    0   0;
23  10  0  300  -300  1  400  1  10  0  0 ...
    0   0  0    0     0  0    0  0 ...
    0   0;
24  10  0  300  -300  1  400  1  10  0  0 ...
    0   0  0    0     0  0    0  0 ...
    0   0;
25  10  0  300  -300  1  400  1  10  0  0 ...
    0   0  0    0     0  0    0  0 ...
    0   0;
26  10  0  300  -300  1  400  1  10  0  0 ...
    0   0  0    0     0  0    0  0 ...
    0   0;
27  10  0  300  -300  1  400  1  10  0  0 ...
    0   0  0    0     0  0    0  0 ...
    0   0;
28  10  0  300  -300  1  400  1  10  0  0 ...
    0   0  0    0     0  0    0  0 ...
    0   0;
29  10  0  300  -300  1  400  1  10  0  0 ...
    0   0  0    0     0  0    0  0 ...
    0   0;
30  10  0  300  -300  1  400  1  10  0  0 ...
    0   0  0    0     0  0    0  0 ...
    0   0;
31  10  0  300  -300  1  400  1  10  0  0 ...
    0   0  0    0     0  0    0  0 ...
    0   0;
32  10  0  300  -300  1  400  1  10  0  0 ...
    0   0  0    0     0  0    0  0 ...
    0   0;
33  10  0  300  -300  1  400  1  10  0  0 ...
    0   0  0    0     0  0    0  0 ...
    0   0;
34  10  0  300  -300  1  400  1  10  0  0 ...
    0   0  0    0     0  0    0  0 ...
    0   0;
35  10  0  300  -300  1  400  1  10  0  0 ...
    0   0  0    0     0  0    0  0 ...
```

```
        0          0;
    36  10  0 300       -300     1      400      1         10            0        0 ...
        0   0         0        0        0        0            0        0          ...
        0          0;
    37  10  0 300       -300     1      400      1         10            0        0 ...
        0   0         0        0        0        0            0        0          ...
        0          0;
    38  10  0 300       -300     1      400      1         10            0        0 ...
        0   0         0        0        0        0            0        0          ...
        0          0;
    39  10  0 300       -300     1      400      1         10            0        0 ...
        0   0         0        0        0        0            0        0          ...
        0          0;
    40  10  0 300       -300     1      400      1         10            0        0 ...
        0   0         0        0        0        0            0        0          ...
        0          0;
    41  10  0 300       -300     1      400      1         10            0        0 ...
        0   0         0        0        0        0            0        0          ...
        0          0;
];

%% branch data
% fbus   tbus   r            x            b          rateA  rateB  rateC  ratio ...
    angle  status   angmin   angmax
mpc.branch = [
  2         1         0.0130089 0.0109624 0.0007527    50       50        50     ...
      0          0        1          -360  360;
  3         2         0.0260178 0.0124048 0.0006158    50       50        50     ...
      0          0        1          -360  360;
  4         3         0.0328645 0.0126933 0.0005816    50       50        50     ...
      0          0        1          -360  360;
  5         4         0.0328645 0.0126933 0.0005816    50       50        50     ...
      0          0        1          -360  360;
    6         1         0.0130089 0.0109624 0.0007527    50       50        50 ...
          0          0        1          -360  360;
    7         6         0.0260178 0.0124048 0.0006158    50       50        50 ...
          0          0        1          -360  360;
    8         7         0.0328645 0.0126933 0.0005816    50       50        50 ...
          0          0        1          -360  360;
    9         8         0.0328645 0.0126933 0.0005816    50       50        50 ...
          0          0        1          -360  360;
    10        1         0.0130089 0.0109624 0.0007527    50       50        50 ...
          0          0        1          -360  360;
    11        10        0.0260178 0.0124048 0.0006158    50       50        50 ...
          0          0        1          -360  360;
    12        11        0.0328645 0.0126933 0.0005816    50       50        50 ...
          0          0        1          -360  360;
    13        12        0.0328645 0.0126933 0.0005816    50       50        50 ...
          0          0        1          -360  360;
    14        1         0.0130089 0.0109624 0.0007527    50       50        50 ...
          0          0        1          -360  360;
    15        14        0.0260178 0.0124048 0.0006158    50       50        50 ...
          0          0        1          -360  360;
    16        15        0.0328645 0.0126933 0.0005816    50       50        50 ...
          0          0        1          -360  360;
    17        16        0.0328645 0.0126933 0.0005816    50       50        50 ...
          0          0        1          -360  360;
    18        1         0.0130089 0.0109624 0.0007527    50       50        50 ...
          0          0        1          -360  360;
```

```
    19      18      0.0260178 0.0124048 0.0006158    50       50        50 ...
            0       0         1         -360 360;
    20      19      0.0328645 0.0126933 0.0005816    50       50        50 ...
            0       0         1         -360 360;
    21      20      0.0328645 0.0126933 0.0005816    50       50        50 ...
            0       0         1         -360 360;
    22       1      0.0130089 0.0109624 0.0007527    50       50        50 ...
            0       0         1         -360 360;
    23      22      0.0260178 0.0124048 0.0006158    50       50        50 ...
            0       0         1         -360 360;
    24      23      0.0328645 0.0126933 0.0005816    50       50        50 ...
            0       0         1         -360 360;
    25      24      0.0328645 0.0126933 0.0005816    50       50        50 ...
            0       0         1         -360 360;
    26       1      0.0130089 0.0109624 0.0007527    50       50        50 ...
            0       0         1         -360 360;
    27      26      0.0260178 0.0124048 0.0006158    50       50        50 ...
            0       0         1         -360 360;
    28      27      0.0328645 0.0126933 0.0005816    50       50        50 ...
            0       0         1         -360 360;
    29      28      0.0328645 0.0126933 0.0005816    50       50        50 ...
            0       0         1         -360 360;
    30       1      0.0130089 0.0109624 0.0007527    50       50        50 ...
            0       0         1         -360 360;
    31      30      0.0260178 0.0124048 0.0006158    50       50        50 ...
            0       0         1         -360 360;
    32      31      0.0328645 0.0126933 0.0005816    50       50        50 ...
            0       0         1         -360 360;
    33      32      0.0328645 0.0126933 0.0005816    50       50        50 ...
            0       0         1         -360 360;
    34       1      0.0130089 0.0109624 0.0007527    50       50        50 ...
            0       0         1         -360 360;
    35      34      0.0260178 0.0124048 0.0006158    50       50        50 ...
            0       0         1         -360 360;
    36      35      0.0328645 0.0126933 0.0005816    50       50        50 ...
            0       0         1         -360 360;
    37      36      0.0328645 0.0126933 0.0005816    50       50        50 ...
            0       0         1         -360 360;
    38       1      0.0130089 0.0109624 0.0007527    50       50        50 ...
            0       0         1         -360 360;
    39      38      0.0260178 0.0124048 0.0006158    50       50        50 ...
            0       0         1         -360 360;
    40      39      0.0328645 0.0126933 0.0005816    50       50        50 ...
            0       0         1         -360 360;
    41      40      0.0328645 0.0126933 0.0005816    50       50        50 ...
            0       0         1         -360 360;

];

%%-----  OPF Data  -----%%
```